References

1. Kawashima S, Yokoyama M. Dysfunction of endothelial nitric oxide synthase and atherosclerosis. *Arterioscler Thromb Vasc Biol.* 2004;24(6):998-1005.
2. Knowles JW, Reddick RL, Jennette JC, Shesely EG, Smithies O, Maeda N. Enhanced atherosclerosis and kidney dysfunction in eNOS(−/−)Apoe(−/−) mice are ameliorated by enalapril treatment. *J Clin Invest.* 2000;105(4):451-458.
3. Chen J, Kuhlencordt PJ, Astern J, Gyurko R, Huang PL. Hypertension does not account for the accelerated atherosclerosis and development of aneurysms in male apolipoprotein e/endothelial nitric oxide synthase double knockout mice. *Circulation.* 2001;104(20):2391-2394.
4. Kuhlencordt PJ, Gyurko R, Han F, et al. Accelerated atherosclerosis, aortic aneurysm formation, and ischemic heart disease in apolipoprotein E/endothelial nitric oxide synthase double-knockout mice. *Circulation.* 2001;104(4):448-454.
5. Searles CD. Transcriptional and posttranscriptional regulation of endothelial nitric oxide synthase expression. *Am J Physiol Cell Physiol.* 2006;291(5):C803-C816.
6. Fulton D, Gratton JP, Sessa WC. Post-translational control of endothelial nitric oxide synthase: why isn't calcium/calmodulin enough? *J Pharmacol Exp Ther.* 2001;299(3):818-824.
7. Anderson HD, Rahmutula D, Gardner DG. Tumor necrosis factor-alpha inhibits endothelial nitric-oxide synthase gene promoter activity in bovine aortic endothelial cells. *J Biol Chem.* 2004;279(2):963-969.
8. Neumann P, Gertzberg N, Johnson A. TNF-alpha induces a decrease in eNOS promoter activity. *Am J Physiol Lung Cell Mol Physiol.* 2004;286(2):L452-:459.
9. Alonso J, Sanchez de Miguel L, Monton M, Casado S, Lopez-Farre A. Endothelial cytosolic proteins bind to the 3′ untranslated region of endothelial nitric oxide synthase mRNA: regulation by tumor necrosis factor alpha. *Mol Cell Biol.* 1997;17(10):5719-5726.
10. Ross R. Atherosclerosis–an inflammatory disease. *N Engl J Med.* 1999;340(2):115-126.
11. Hansson GK, Libby P. The immune response in atherosclerosis: a double-edged sword. *Nat Rev Immunol.* 2006;6(7):508-519.
12. Libby P, Theroux P. Pathophysiology of coronary artery disease. *Circulation.* 2005;111(25):3481-3488.
13. Tedgui A, Mallat Z. Cytokines in atherosclerosis: pathogenic and regulatory pathways. *Physiol Rev.* 2006;86(2):515-581.
14. Rahman A, Bando M, Kefer J, Anwar KN, Malik AB. Protein kinase C-activated oxidant generation in endothelial cells signals intercellular adhesion molecule-1 gene transcription. *Mol Pharmacol.* 1999;55(3):575-583.
15. Javaid K, Rahman A, Anwar KN, Frey RS, Minshall RD, Malik AB. Tumor necrosis factor-alpha induces early-onset endothelial adhesivity by protein kinase Czeta-dependent activation of intercellular adhesion molecule-1. *Circ Res.* 2003;92(10):1089-1097.
16. Garin G, Abe J, Mohan A, et al. Flow antagonizes TNF-alpha signaling in endothelial cells by inhibiting caspase-dependent PKC zeta processing. *Circ Res.* 2007;101(1):97-105.
17. Magid R, Davies PF. Endothelial protein kinase C isoform identity and differential activity of PKC-zeta in an athero-susceptible region of porcine aorta. *Circ Res.* 2005;97(5):443-449.
18. Moscat J, Diaz-Meco MT, Wooten MW. Of the atypical PKCs, Par-4 and p62: recent understandings of the biology and pathology of a PB1-dominated complex. *Cell Death Differ.* 2009;16(11):1426-137.
19. Atkins GB, Wang Y, Mahabeleshwar GH, et al. Hemizygous deficiency of Kruppel-like factor 2 augments experimental atherosclerosis. *Circ Res.* 2008;103(7):690-693.
20. Berk BC. Atheroprotective signaling mechanisms activated by steady laminar flow in endothelial cells. *Circulation.* 2008;117(8):1082-1089.
21. Yan C, Takahashi M, Okuda M, Lee JD, Berk BC. Fluid shear stress stimulates big mitogen-activated protein kinase 1 (BMK1) activity in endothelial cells. Dependence on tyrosine kinases and intracellular calcium. *J Biol Chem.* 1999;274(1):143-150.
22. Parmar KM, Larman HB, Dai G, et al. Integration of flow-dependent endothelial phenotypes by Kruppel-like factor 2. *J Clin Invest.* 2006;116(1):49-58.
23. Dekker RJ, van Soest S, Fontijn RD, et al. Prolonged fluid shear stress induces a distinct set of endothelial cell genes, most specifically lung Kruppel-like factor (KLF2). *Blood.* 2002;100(5):1689-1698.
24. Akaike M, Che W, Marmarosh NL, et al. The hinge-helix 1 region of peroxisome proliferator-activated receptor gamma1 (PPARgamma1) mediates interaction with extracellular signal-regulated kinase 5 and PPARgamma1 transcriptional activation: involvement in flow-induced PPARgamma activation in endothelial cells. *Mol Cell Biol.* 2004;24(19):8691-8704.
25. Woo CH, Shishido T, McClain C, et al. Extracellular signal-regulated kinase 5 SUMOylation antagonizes shear stress-induced antiinflammatory response and endothelial nitric oxide synthase expression in endothelial cells. *Circ Res.* 2008;102(5):538-545.
26. Abe J, Takahashi M, Ishida M, Lee JD, Berk BC. c-Src is required for oxidative stress-mediated activation of big mitogen-activated protein kinase 1. *J Biol Chem.* 1997;272(33):20389-20394.
27. Abe J, Kusuhara M, Ulevitch RJ, Berk BC, Lee JD. Big mitogen-activated protein kinase 1 (BMK1) is a redox-sensitive kinase. *J Biol Chem.* 1996;271(28):16586-16590.
28. Diaz-Meco MT, Berra E, Municio MM, et al. A dominant negative protein kinase C zeta subspecies blocks NF-kappa B activation. *Mol Cell Biol.* 1993;13(8):4770-4775.
29. Nunes GL, Sgoutas DS, Redden RA, et al. Combination of vitamins C and E alters the response to coronary balloon injury in the pig. *Arterioscler Thromb Vasc Biol.* 1995;15(1):156-165.
30. Won D, Zhu SN, Chen M, et al. Relative reduction of endothelial nitric-oxide synthase expression and transcription in atherosclerosis-prone regions of the mouse aorta and in an in vitro model of disturbed flow. *Am J Pathol.* 2007;171(5):1691-1704.
31. Atkins GB, Jain MK. Role of Kruppel-like transcription factors in endothelial biology. *Circ Res.* 2007;100(12):1686-1695.
32. Woo CH, Massett MP, Shishido T, et al. ERK5 activation inhibits inflammatory responses via peroxisome proliferator-activated receptor delta (PPARdelta) stimulation. *J Biol Chem.* 2006;281(43):32164-32174.
33. Barath P, Fishbein MC, Cao J, Berenson J, Helfant RH, Forrester JS. Detection and localization of tumor necrosis factor in human atheroma. *Am J Cardiol.* 1990;65(5):297-302.
34. Harry BL, Sanders JM, Feaver RE, et al. Endothelial cell PECAM-1 promotes atherosclerotic lesions in areas of disturbed flow in ApoE-deficient mice. *Arterioscler Thromb Vasc Biol.* 2008;28(11):2003-2008.
35. Pi X, Yan C, Berk BC. Big mitogen-activated protein kinase (BMK1)/ERK5 protects endothelial cells from apoptosis. *Circ Res.* 2004;94(3):362-369.
36. Xiao N, Yin M, Zhang L, et al. Tumor necrosis factor-alpha deficiency retards early fatty-streak lesion by influencing the expression of inflammatory factors in apoE-null mice. *Mol Genet Metab.* 2009;96(4):239-244.
37. Rus HG, Niculescu F, Vlaicu R. Tumor necrosis factor-alpha in human arterial wall with atherosclerosis. *Atherosclerosis.* 1991;89(2-3):247-254.
38. Branen L, Hovgaard L, Nitulescu M, Bengtsson E, Nilsson J, Jovinge S. Inhibition of tumor necrosis factor-alpha reduces atherosclerosis in apolipoprotein E knockout mice. *Arterioscler Thromb Vasc Biol.* 2004;24(11):2137-2142.
39. Canault M, Peiretti F, Mueller C, et al. Exclusive expression of transmembrane TNF-alpha in mice reduces the inflammatory response in early lipid lesions of aortic sinus. *Atherosclerosis.* 2004;172(2):211-218.
40. Ohta H, Wada H, Niwa T, et al. Disruption of tumor necrosis factor-alpha gene diminishes the development of atherosclerosis in ApoE-deficient mice. *Atherosclerosis.* 2005;180(1):11-17.
41. Yamawaki H, Pan S, Lee RT, Berk BC. Fluid shear stress inhibits vascular inflammation by decreasing thioredoxin-interacting protein in endothelial cells. *J Clin Invest.* 2005;115(3):733-738.
42. Averna M, Stifanese R, De Tullio R, et al. Functional role of HSP90 complexes with endothelial nitric-oxide synthase (eNOS) and calpain on nitric oxide generation in endothelial cells. *J Biol Chem.* 2008;283(43):29069-29076.
43. Dong Y, Wu Y, Wu M, et al. Activation of protease calpain by oxidized and glycated LDL increases the degradation of endothelial nitric oxide synthase. *J Cell Mol Med.* 2009;13(9A):2899-2910.
44. Passerini AG, Polacek DC, Shi C, et al. Coexisting proinflammatory and antioxidative endothelial transcription profiles in a disturbed flow region of the adult porcine aorta. *Proc Natl Acad Sci U S A.* 2004;101(8):2482-2487.

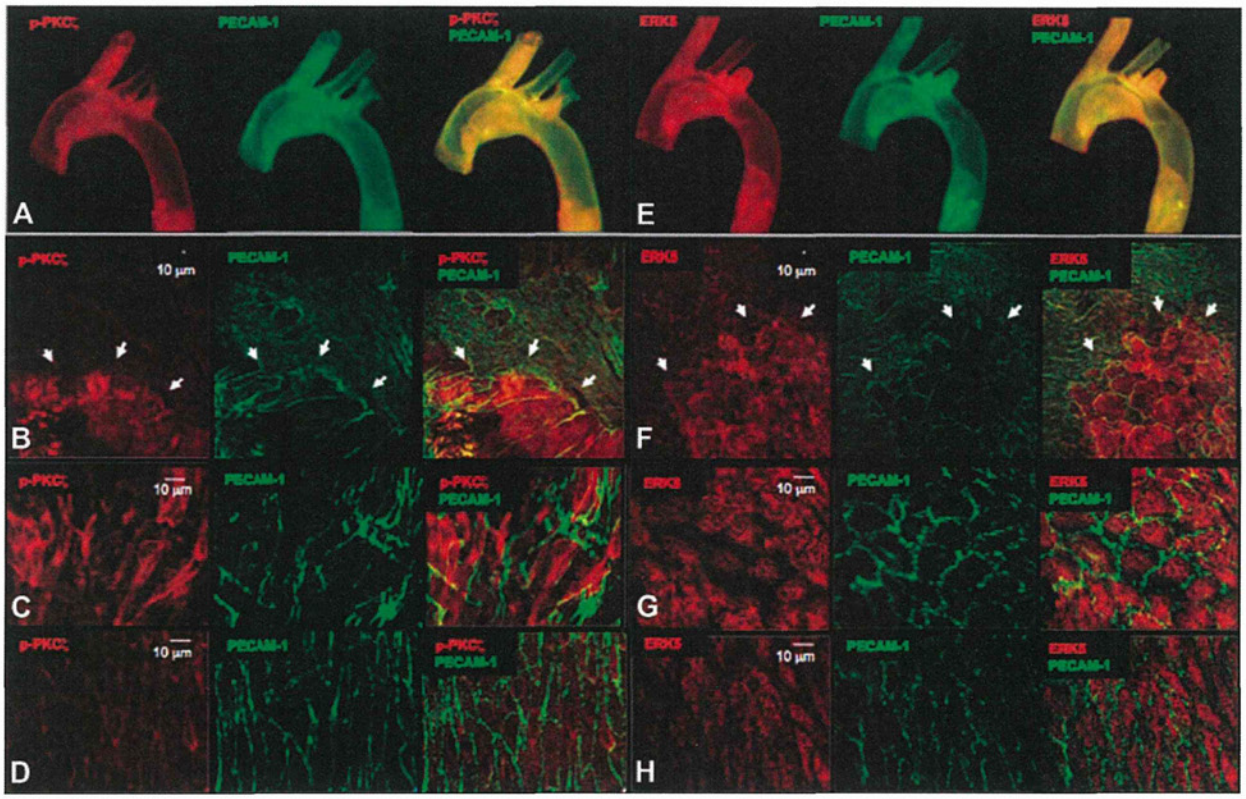

Figure 6. PKCζ activation and ERK5 expression in the ApoE$^{-/-}$ mouse. Aortas from 12-week-old ApoE$^{-/-}$ mice were harvested for qualitative analysis of PKCζ activation (A-D red) and ERK5 expression (E-H red). The differential PKCζ activation or ERK5 expression is evident in the images of the whole aortic mount (4× lens; A,E), in the en face analysis of the aortic arch (20× lens; B,F), and specifically in the athero-prone (C,G; 60× lens) and athero-protected (D, H; 60× lens) areas of the aortic arch. EC morphology was changed in the early atherosclerosis regions (B,F; arrowheads) where ECs are stretched and may have lost PECAM-1 staining (green) at some cell junctions. Bar = 10 μm.

suggesting a potential compensatory effect. This finding is consistent with the observations of Passerini et al[44] who observed by microarray analysis of athero-prone regions that both atherosclerosis-susceptible (proinflammatory, prothrombotic) and atherosclerosis-protective (antioxidant and antithrombotic) gene expression were up-regulated.

In conclusion, we believe that PKCζ is a proatherogenic effector in ECs and that it could be an innovative therapeutic target to improve endothelial dysfunction.

Acknowledgments

We thank Maria Antonietta Belisario for her support and valuable advice. We thank the Aab Cardiovascular Research Institute members for useful suggestions, in particular Dietrich Machleder, Eugene Chang, and Weiye Wang for great help and Tamlyn Thomas, Chelsea Wong, and Thomas Spangenberg for technical assistance.

This work was supported by National Institutes of Health (grants HL-064839 and HL-077789, B.C.B.; HL-088637, HL-064839, and HL-077789, J.A.; and HL-064839 and HL-077789, K.F.); the internal grant of the University of Salerno (P.N.); and the American Heart Association (postdoctoral fellowship 0625957T, Scientist Development Grant 0930360N; C.-H.W.).

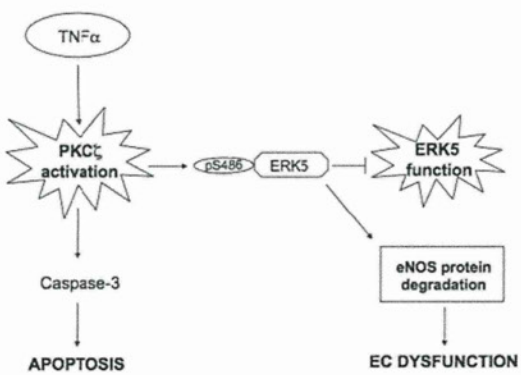

Figure 7. A scheme describing the PKCζ-mediated cross talk between the TNFα (proinflammatory) and ERK5 (anti-inflammatory) pathways.

Authorship

Contribution: P.N. contributed to the design of the experiments, performed the experiments, and generated the manuscript and figures; J.A. and K.F. contributed to discussions and design of experiments and critically edited the paper; C.-H.W. helped the design of the experiments and performed experiments; K.S., H.L., J.-D.L., and K.-S.H. contributed to discussions; C.M. and J.-H.L. performed experiments; M.R.O. performed mouse colony management and genotyping; and B.C.B. supervised the project, contributed to the design of the experiments, and edited the manuscript.

Conflict-of-interest disclosure: The authors declare no competing financial interests.

Correspondence: Bradford C. Berk, Aab Cardiovascular Research Institute, 601 Elmwood Ave, Box CVRI, University of Rochester School of Medicine and Dentistry, Rochester, NY 14642; e-mail: bradford_berk@urmc.rochester.edu.

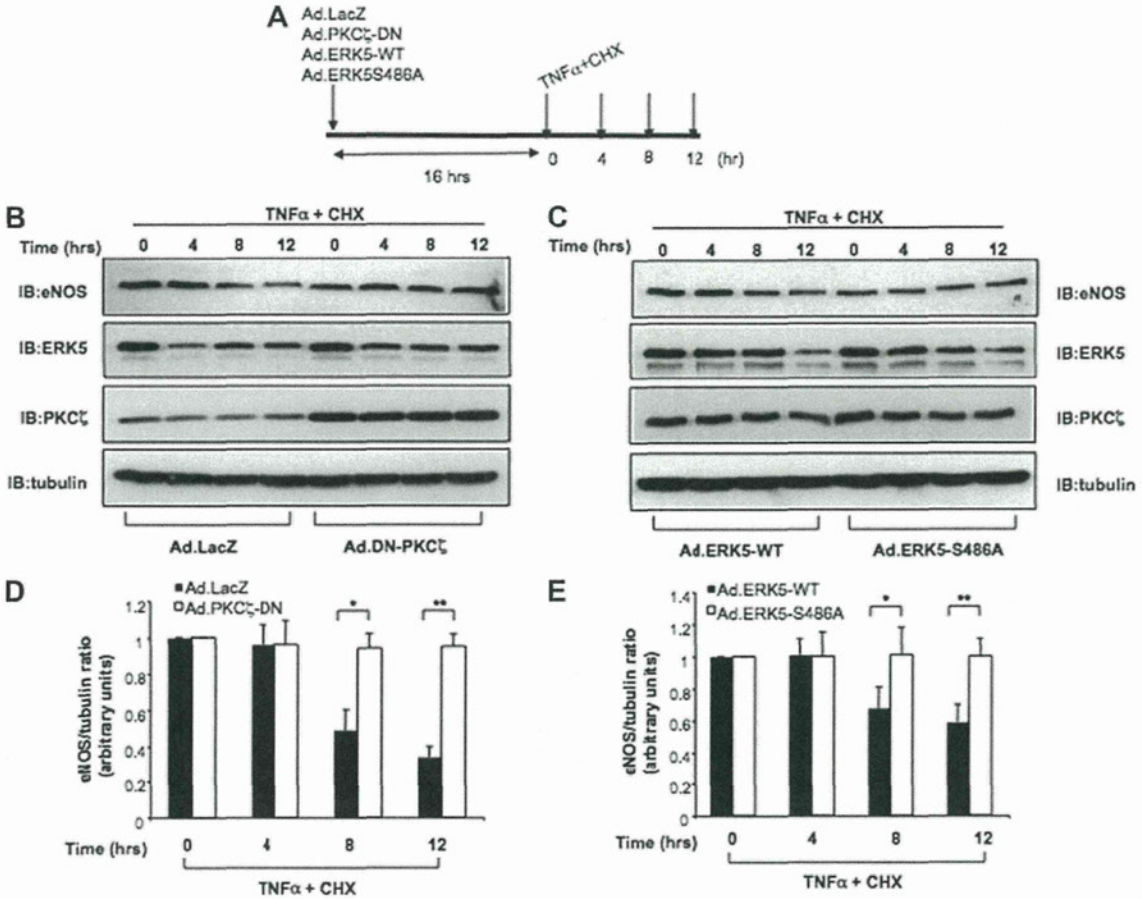

Figure 5. Role of PKCζ in eNOS protein stability. (A) Schematic diagram showing experimental protocol. (B-C) Ad.DN-PKCζ and Ad.ERK5-S486A increase eNOS protein stability. HUVECs were infected with Ad.LacZ (control) or Ad.DN-PKCζ (B) and Ad.ERK5-WT or Ad.ERK5-S486A (C). Sixteen hours later, the cells were incubated with TNFα 10 ng/mL plus the protein synthesis inhibitor cycloheximide (CHX; 10 μg/mL). HUVECs were harvested after 0, 4, 8 and 12 hours of treatment, and Western blots were performed with eNOS, PKCζ, ERK5, and tubulin antibodies. (D-E) Western blots were quantified by densitometry by setting the time zero to 1.0. Data presented are from a representative experiment of at least 3 independent experiments. $^*P < .1$; $^{**}P < .05$.

caspase-3.[16] Recently, eNOS expression was shown to be positively regulated in ECs by a MEK/ERK5/KLF2 pathway.[22] Because we demonstrated that ERK5 was activated by s-flow and protected ECs from apoptosis,[35] we hypothesized that PKCζ might negatively regulate ERK5 and thereby decrease eNOS expression. Furthermore, because both PKCζ and MEK5 contain a PB1 domain, a well-characterized protein-protein interaction domain, we expected that PKCζ inhibition might be by a direct effect on MEK5. However, we found that PKCζ bound directly to ERK5. Furthermore, the ERK5 binding site was within the catalytic domain of PKCζ, not the PB1 domain. Interestingly, we found that ERK5 is not only a binding partner of PKCζ but is also a substrate of this kinase. Our mutational analysis showed that PKCζ phosphorylates ERK5 at a previously uncharacterized phosphorylation site (S486). Phosphorylation of S486 was necessary for the decrease in eNOS protein stability, although the precise mechanism will require future studies.

We used TNFα as an agonist to stimulate ECs because TNFα has been shown to play an important role during the inflammatory process of atherosclerosis. In particular, TNFα deficiency retards fatty-streak lesion formation by down-regulating the expression of proatherogenic inflammatory factors.[36] TNFα has been detected in atherosclerotic lesions throughout all stages of human atherosclerosis[33,37] and was found to be associated with atherosclerosis in mouse models.[38,39] Mice deficient in both ApoE$^{-/-}$ and TNFα displayed less advanced atherosclerosis than ApoE$^{-/-}$ mice.[38,40] In addition, many features of EC dysfunction are mimicked by the inflammatory cytokine TNFα. For example, TNFα stimulation activates PKCζ,[15] induces adhesion molecule expression,[41] and decreases eNOS expression.[7-9] The mechanism for TNFα-mediated inhibition of eNOS expression has been thought to be primarily transcriptional.[7,8] However, a role for a decrease in mRNA stability has also been elucidated.[9] Surprisingly, our data predict that a posttranslational modification of eNOS protein by PKCζ targets eNOS for degradation. Several mechanisms have been proposed for eNOS degradation with calcium-dependent calpain-mediated degradation being most prominent.[42,43] Further studies will be required to define the molecular nature of the PKCζ-ERK5 pathway described here.

To understand the importance of the proposed PKCζ-ERK5 mechanism during early atherosclerotic events, we performed en face staining of aortas from ApoE$^{-/-}$ mice. Specifically, we showed that endothelial PKCζ phosphorylation and activation were increased in the athero-susceptible region of the aortic arch (d-flow region). In the in vivo system of the chow fed ApoE$^{-/-}$ mouse, the endothelium in the lesser curvature of the aorta had distinctively large ECs filled with vacuoles that were positive for p-PKCζ immunostaining. These EC changes, which were probably a consequence of intimal leukocyte accumulation, were not observed in regions that experienced s-flow. Note that the expression of ERK5, which has athero-protective effects, was also up-regulated in the same ECs that showed the highest level of p-PKCζ,

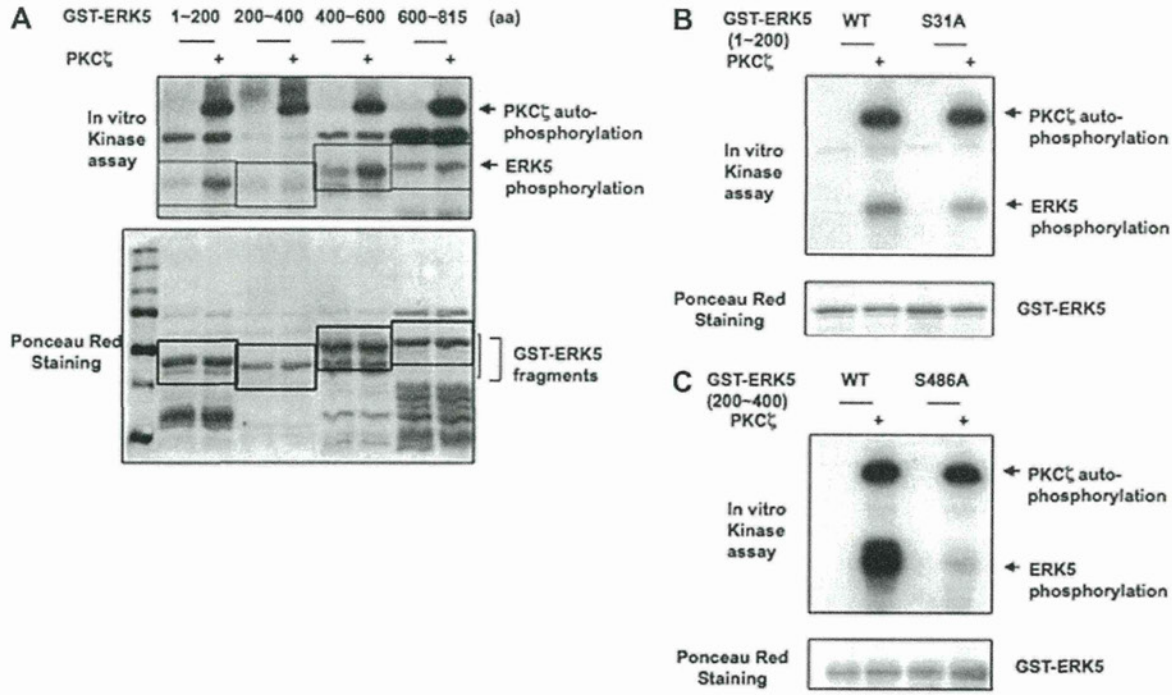

Figure 4. PKCζ directly phosphorylates ERK5 in vitro. (A) To determine direct PKCζ-induced ERK5 phosphorylation, we performed an in vitro kinase assay with 4 different GST-ERK5 fragments as substrate. In vitro kinase assay shows ^{32}P incorporation into 2 GST-ERK5 fragments (amino acids 100 ~ 200 and 400 ~ 600) but not into the others (amino acids 200 ~ 400 and 600 ~ 816). Ponceau staining shows the position of the proteins after separation by SDS-PAGE and near equal expression. (B-C) Characterization of PKCζ phosphorylation sites. In vitro kinase assay was performed with ERK5-WT fragment (aa1-200 or aa400-600) and ERK5 fragment with S31A (B) or S486A (C) mutations in the presence of recombinant PKCζ. Mutation of the serine 486 to alanine in GST-ERK5 200-600 ablated PKCζ-mediated ERK5 phosphorylation. Data presented are from a representative experiment of at least 3 independent experiments.

This athero-prone area is characterized by d-flow in contrast to the relatively protected greater curvature that is characterized by s-flow. Our data provide a novel insight into the mechanism by which eNOS expression is reduced in areas of d-flow as reported.[30] Our current study predicts that eNOS degradation in areas of d-flow is the result of phosphorylation of ERK5 by PKCζ. To further elucidate the importance of PKCζ activation in eNOS degradation, we studied an atherosclerotic disease model, the ApoE$^{-/-}$ C57BL/6J mouse. En face preparations of aortas were immunostained for p-PKCζ (Thr410) and PECAM-1 (as an EC marker) and studied with a confocal laser scanning microscope. Low-magnification (4×) images of representative mouse aortas are shown in Figure 6A. There was increased staining for p-PKCζ in atherosclerotic lesions present in the athero-prone region (lesser curvature) compared with athero-protected region (greater curvature). Increased magnification (10×) images show that p-PKCζ was specifically increased in ECs that exhibited abnormal morphology characterized by increased size, loss of polygonal shape, and appearance of gaps between cells (Figure 6B). p-PKCζ appeared to be localized to the perinuclear area and did not colocalize with PECAM-1 (Figure 6B). A direct comparison of the athero-prone region (Figure 6C) with the athero-protected region (Figure 6D) showed that cells with abnormal morphology were the ones that most highly expressed p-PKCζ. Analysis of PECAM-1 showed that it was also more highly expressed in the d-flow region (lesser curvature) than in the s-flow-region (greater curvature). This result is consistent with a recent study indicating that PECAM-1 contributes to atherosclerosis lesion formation in regions of d-flow in ApoE$^{-/-}$ mice.[34]

Unfortunately, we were unable to develop an antibody that could detect phospho-S486 ERK5, so we studied total ERK5 expression. Analysis of ERK5 expression showed that it was also more highly expressed in athero-prone regions compared with athero-protected regions (Figure 6E). Higher magnification images (Figure 6F) showed that cells that highly expressed ERK5 were the same cells that exhibited abnormal morphology and appeared to overlap with those that highly expressed p-PKCζ (compare Figure 6F with 6B). Interestingly ERK5 appeared to be cytoplasmic as well as nuclear in both normal- and abnormal-appearing ECs (Figure 6G). Direct comparison of the athero-prone region (Figure 6G) to the athero-protected region (Figure 6H) showed no obvious difference in ERK5 subcellular localization. There was clearly a significant increase in ERK5 expression in the d-flow region that corresponded to the increase in p-PKCζ (compare Figure 6G with 6C). These data suggest a potential proatherogenic role for endothelial PKCζ activation and PKCζ-mediated phosphorylation of ERK5.

Discussion

The main finding of the present study is that activation of PKCζ phosphorylates ERK5 and by inhibiting ERK5 function decreases eNOS protein expression in ECs. Specifically, we demonstrated that PKCζ binds and phosphorylates ERK5 at S486, and these events are required to increase eNOS protein degradation (Figure 7). Furthermore, we observed in vivo that PKCζ activity was up-regulated in athero-prone regions of the mouse aorta exposed to d-flow. These results define a new mechanism for endothelial dysfunction and atherosclerosis progression.

PKCζ activity was shown to be up-regulated in the d-flow region of the pig aorta by Magid and Davies,[17] but the mechanism by which PKCζ contributed to atherosclerosis susceptibility was not described. Previously, we found that PKCζ mediated TNFα-dependent EC apoptosis and was required for activation of

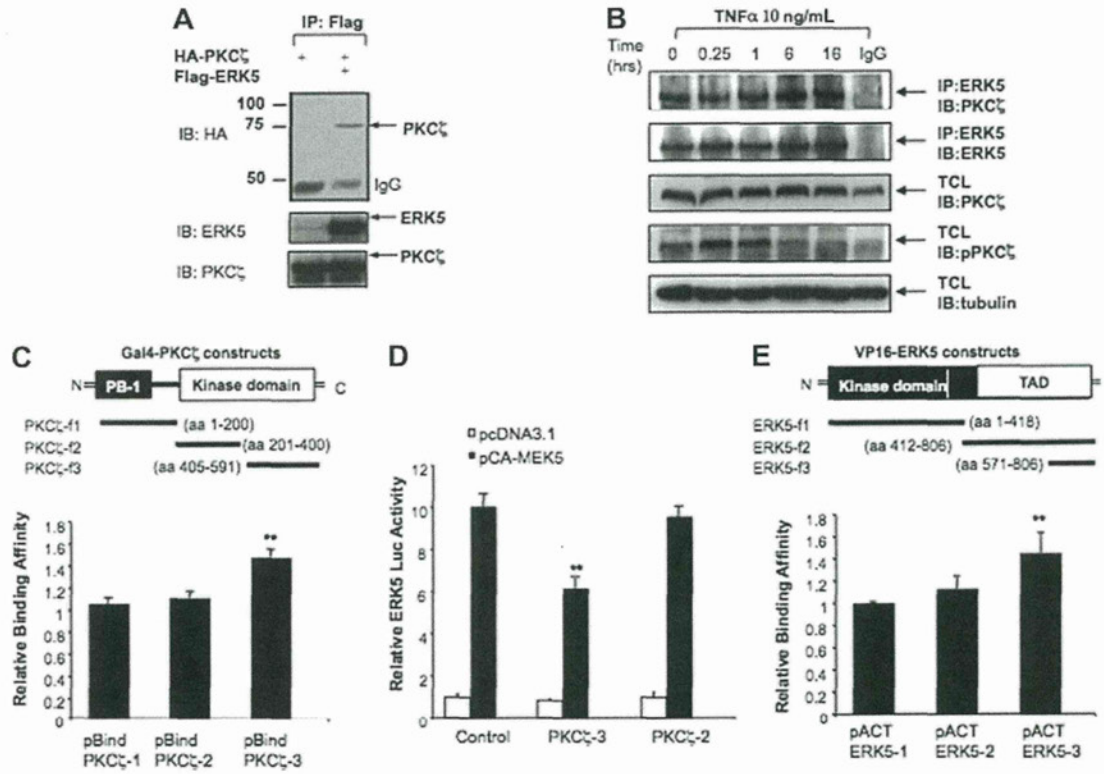

Figure 3. PKCζ interacts with ERK5. (A) ERK5 binds to PKCζ in vitro. HeLa cells were cotransfected with HA-PKCζ and pcDNA3 or Flag-ERK5 for 24 hours and subjected to immunoprecipitation with Flag antibody, followed by Western blot analysis with HA antibody. Expression of ERK5 and PKCζ was detected by Western blotting with specific antibodies. (B) TNFα slightly increases PKCζ-ERK5 binding. Subconfluent cocultures of HUVECs were treated for different time points with TNFα 10 ng/mL. The interaction of endogenous PKCζ with endogenous ERK5 was evaluated by immunoprecipitating 400 μg of total cell lysate with ERK5 antibody, and the immunoprecipitates were analyzed by immunoblotting with PKCζ antibody. Essentially identical results were obtained in 2 other experiments. (C,E) The COOH-terminus regions of PKCζ and ERK5 are critical for the ERK5-PKCζ interaction. HUVECs were transfected with plasmids expressing wild-type VP16-ERK5 with Gal4-PKCζ fragments (C) or wild-type Gal4-PKCζ with VP16-ERK5 fragments (E) as indicated, and luciferase activity was evaluated 24 hours after transfection. (D) PKCζ fragment able to bind ERK5 inhibits ERK5 transactivation. HUVECs were transfected with pBIND-ERK5 and Gal4-dependent (pG5-Luc) reporter gene with or without pcDNA3-CA-MEK5α with PKCζ-3 and PKCζ-2 fragments. Luciferase activity was measured after 24 hours of incubation. Data are mean ± SD of 3 experiments performed in triplicate. $^{**}P < .05$.

Role of PKCζ and PKCζ-mediated ERK5 phosphorylation in the regulation of eNOS protein stability

We showed earlier that s-flow–induced up-regulation of eNOS expression was inhibited by TNFα and that this inhibition was abrogated by expressing Ad.DN-PKCζ (Figure 1C-D), indicating that PKCζ is involved in down-regulating eNOS expression. Indeed, when we cotransfected Chinese hamster ovary cells with eNOS cDNA and the constitutively active PKCζ (CATζ), eNOS expression was dose-dependently inhibited (Supplemental Figure 2A-B), thus confirming the inhibitory role of PKCζ in eNOS expression. Because s-flow has been shown to induce eNOS mRNA expression by activating the ERK5/MEF2/KLF2 pathway[22] and because activation of PKCζ inhibits ERK5 transactivation (Figure 2B), it is possible that TNFα inhibits KLF2 and eNOS promoter activity by activating PKCζ. To test this possibility, HUVECs were transduced with Ad.DN-PKCζ and transfected with eNOS or pKLF2 promoter, exposed to TNFα or s-flow, and promoter activities were assayed by luciferase activity. In control cells, TNFα reduced eNOS and KLF2 promoter activity and mRNA expression under both static and flow conditions (supplemental Figure 3). Interestingly, expression of Ad.DN-PKCζ did not prevent the down-regulation of eNOS and KLF2 promoter activity and mRNA expression. These data suggest that the recovery of eNOS protein expression by Ad.DN-PKCζ shown in Figure 1C may be due to protein stabilization rather than increased transcription.

To determine the mechanism by which PKCζ regulates eNOS stability, we first examined TNFα-mediated eNOS degradation by PKCζ activation. HUVECs were transduced with Ad.LacZ or Ad.DN-PKCζ and treated with cycloheximide (CHX) plus TNFα for 0 to 12 hours as indicated (Figure 5A). Then, eNOS expression levels were analyzed by immunoblotting. In control cells expressing Ad.LacZ, TNFα decreased eNOS expression in the presence of the protein synthesis inhibitor CHX, but cells expressing Ad.DN-PKCζ, which inhibits PKCζ activity, significantly prevented the decrease in eNOS protein levels induced by TNFα (Figure 5B,D). These experiments show that PKCζ negatively regulates eNOS protein levels. Next, to determine the role of PKCζ-mediated ERK5 phosphorylation on eNOS stability, we transduced HUVECs with Ad.ERK5-WT or Ad.ERK5-S486 and repeated the same experiments described above. The expression of ERK5-WT and ERK5-S486A mutant was comparable throughout the time course of the experiment (Figure 5C second panel from top). In cells transduced with Ad.ERK5-WT, endogenous eNOS expression decreased after 12 hours of TNFα and CHX treatment. In contrast, in cells expressing the Ad.ERK5-S486A mutant, TNFα and CHX treatment did not significantly decrease eNOS expression by 12 hours (Figure 5C,E). These results suggest that the TNFα-mediated eNOS destabilization depends on PKCζ-mediated ERK5 phosphorylation.

In situ localization of PKCζ and ERK5 in ApoE$^{-/-}$ mouse aorta

Importantly, increased PKCζ activation at disturbed flow (d-flow) areas such as the lesser curvature of the aorta has been observed.[17]

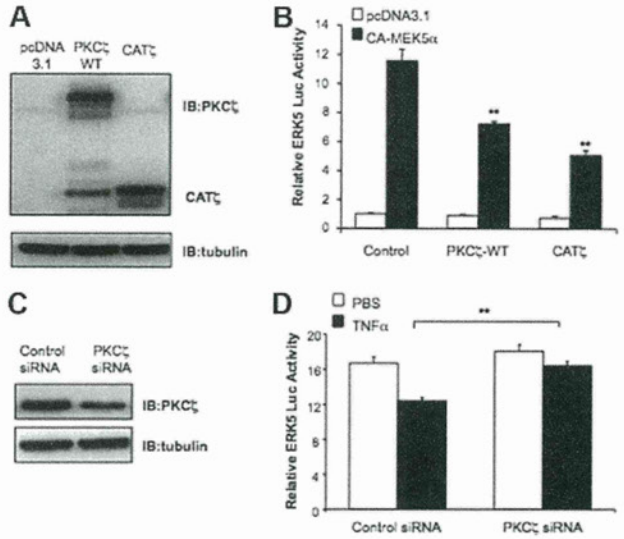

Figure 2. TNFα inhibits ERK5 transactivation by PKCζ. (A) HA-PKCζ-WT and CATζ overexpression was verified with the use of cell lysates probed with anti-PKCζ. (B) PKCζ-WT and CATζ inhibit ERK5 transactivation. HUVECs were transfected with pBIND-ERK5 and Gal4-dependent (pG5-Luc) reporter gene with or without pcDNA3-CA-MEK5α with 0.3 μg of control vector or expression plasmids for PKCζ-WT or CATζ. ERK5 transcriptional activity was evaluated by measuring luciferase activity after 24 hours. (C) PKCζ silencing was confirmed by Western blot analysis. (D) Depletion of PKCζ expression reverses TNFα-mediated inhibition of ERK5 transcriptional activity. HUVECs were pretreated for 24 hours with siRNA targeting PKCζ and then cotransfected with pBIND-ERK5 and Gal4-dependent (pG5-Luc) reporter gene with or without pcDNA3-CA-MEK5α. After 8 hours, cells were treated with 10 ng/mL TNFα, and ERK5 luciferase activity was determined 16 hours later. Results are expressed in arbitrary units normalized to the control (set to 1.0 for each experiment). Data are mean ± SD of 3 experiments performed in triplicate. $^{**}P < .05$.

PKCζ activation by TNFα inhibits ERK5 function

The critical role of the MEK5/ERK5/KLF2 pathway in inhibiting endothelial inflammation and stimulating eNOS expression is well described.[22,25,31-33] To investigate whether PKCζ activation negatively regulates ERK5, we cotransfected HUVECs with PKCζ-WT, CATζ, or the empty vector (pcDNA3.1) with Gal4-ERK5 and constitutively active MEK5 (CA-MEK5α) constructs as indicated (Figure 2), and then performed a luciferase assay. Both PKCζ-WT and CATζ significantly inhibited CA-MEK5α–mediated ERK5 transactivation (Figure 2B).

To inhibit PKCζ activity we used siRNA to reduce PKCζ expression (Figure 2C). To assay the effect of reducing PKCζ we measured ERK5-dependent luciferase activity as described in Figure 2B. ERK5 transactivation was inhibited by TNFα in control siRNA transfected cells and reversed in PKCζ siRNA transfected cells (Figure 2D). These data show a critical role for PKCζ in TNFα-induced inhibition of ERK5 transactivation.

We have previously reported that ERK5 SUMOylation at Lys6 and Lys22 inhibited its transcriptional activity.[25] These data suggest that the inhibition of ERK5 transactivation by TNFα may be due to ERK5 SUMOylation. To test this possibility, we studied the effect of TNFα on ERK5 transactivation in HUVECs expressing ERK5-K6R/K22R (K6/K22R mutant) which cannot undergo SUMOylation.[25] HUVECs were transfected with ERK5-K6/K22R, a Gal4-dependent luciferase reporter gene with or without CA-MEK5α, treated with TNFα, and assayed for luciferase activity. TNFα significantly inhibited ERK5 transactivation in a dose-dependent manner (supplemental Figure 1A, available on the *Blood* Web site; see the Supplemental Materials link at the top of the online article), but we observed no significant effects of the K6/K22R mutant on the TNFα-induced inhibition of ERK5 transactivation (supplemental Figure 1B). To determine whether ERK5 tyrosine phosphorylation at the TEY motif (Thr218/Tyr220; the dual-phosphorylation site) is involved in its down-regulation by TNFα, HUVECs were transduced with Ad.CA-MEK5α to activate ERK5. We found no inhibition of ERK5 phosphorylation at these sites by TNFα (supplemental Figure 1C). These results suggest that TNFα-mediated inhibition of ERK5 transactivation is not due to ERK5 SUMOylation or phosphorylation of the TEY motif.

PKCζ associates directly with ERK5

To determine whether PKCζ inhibition involved direct binding to ERK5, we tested their interaction. We cotransfected HeLa cells with HA-tagged PKCζ and Flag-tagged ERK5, immunoprecipitated with Flag antibody, and assayed for HA-PKCζ in the immunoprecipitates (Figure 3A). Under these conditions there was coprecipitation of PKCζ and ERK5. To investigate the interaction between endogenous PKCζ and ERK5, we stimulated HUVECs with TNFα at the indicated times, and the cell lysates were immunoprecipitated with ERK5 antibody (Figure 3B). We found that PKCζ coimmunoprecipitated with ERK5 under basal conditions (T = 0 hours) and that TNFα stimulation did not significantly increase PKCζ-ERK5 interaction (Figure 3B). These results suggest that PKCζ is constitutively associated with ERK5.

To determine the ERK5 binding site for PKCζ, we used a mammalian 2-hybrid assay in HUVECs. Plasmids containing GAL4-DBD and truncated forms of PKCζ were constructed with the use of the pBIND vector. A plasmid containing VP16-ERK5 was constructed with the use of the pACT vector. Transfection of HUVECs with these constructs, and assay for luciferase activity as a measure of interaction, showed that only cells expressing the C-terminal kinase domain (aa405-591) of PKCζ exhibited increased activity (Figure 3C), indicating that this is the ERK5 binding domain. To study further functional interaction, we transfected cells with CA-MEK5α and the truncated PKCζ constructs (Figure 3D). As expected, PKCζ fragment 3 (aa405-591), but not fragment 2 (aa201-400), significantly decreased ERK5 transactivation (Figure 3D).

To determine the PKCζ binding site for ERK5, we cotransfected HUVECs with Gal4-PKCζ and the truncated forms of VP16-ERK5 constructs. The interaction of these fragments was then assayed by luciferase activity. As shown in Figure 3E, we found that the C-terminal domain (aa571-806) of ERK5 was required for PKCζ-ERK5 association. Because this domain has multiple potential protein association motifs, future studies will be required to define the specific regions necessary for interaction.

PKCζ phosphorylates ERK5

To investigate whether PKCζ phosphorylates ERK5 and, if so, to determine the site(s) of phosphorylation, we generated GST-tagged ERK5 fragments and performed in vitro kinase assay with PKCζ. ERK5 fragments consisting of aa1-200 and aa400-600 were highly phosphorylated by PKCζ (Figure 4A). When we used NetPhosK1.0 software to search for possible phosphorylation sites in the ERK5 sequence, 2 serine residues (S31 and S468) were identified as the most likely phosphorylation targets. GST-ERK5 with either S31A or S486A point mutations were used in the in vitro kinase assay. We found that the S486A point mutation ablated PKCζ-mediated ERK5 phosphorylation (Figure 4C), whereas the S31A mutation did not (Figure 4B). These results indicate that PKCζ phosphorylates S486 of ERK5.

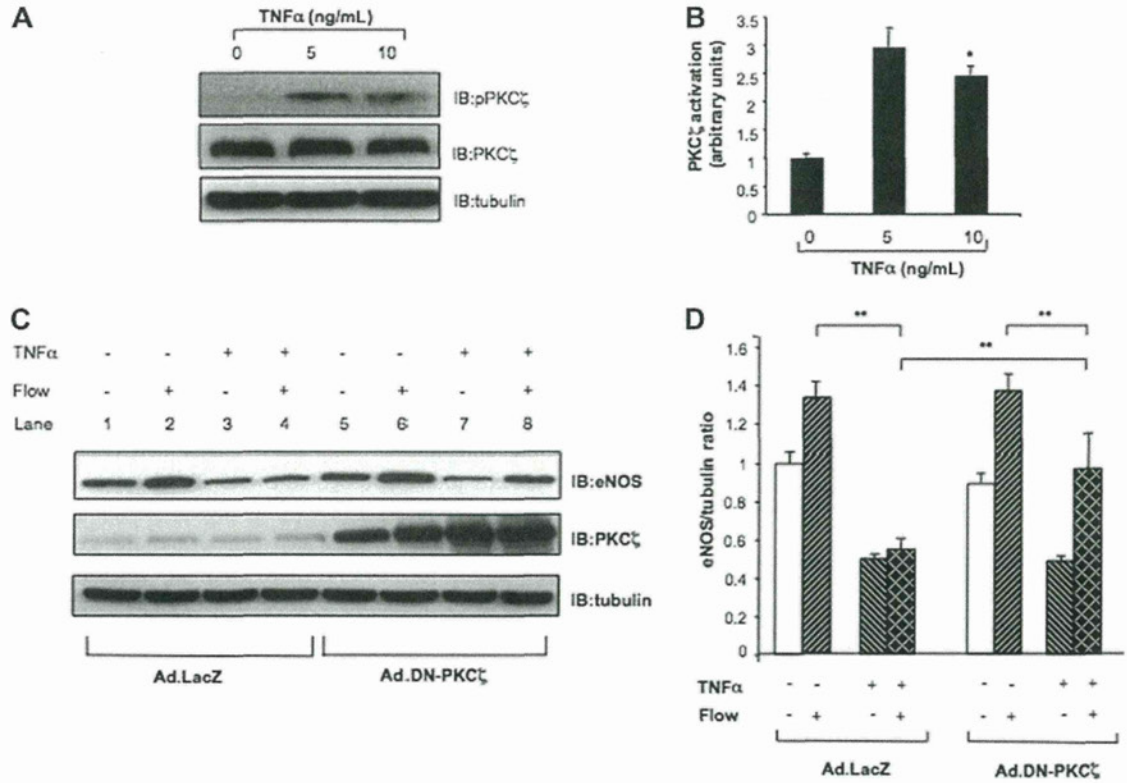

Figure 1. Reducing PKCζ activity by Ad.DN-PKCζ reverses TNFα inhibition of eNOS. (A-B) TNFα increases PKCζ activation/phosphorylation. (A) Confluent BAECs were exposed to TNFα 5 and 10 ng/mL or vehicle alone for 15 minutes. Then, cells were lysed and immunoblotted with p-PKCζ and total PKCζ antibodies, respectively. The amount of proteins loaded in each lane was equal as shown by incubating the same blots with antitubulin antibody. (B) Densitometric analysis of p-PKCζ. Results were normalized by arbitrarily setting the average densitometry of the control to 1.0. Representative blots are shown from 3 separate experiments. $*P < .01$. (C-D) TNFα-mediated eNOS reduction is PKCζ dependent. (C) HUVECs were transfected with Ad.LacZ (control) or Ad.DN-PKCζ. After 16 hours cells were treated with TNFα or vehicle and then exposed to flow (shear stress = 12 dyn/cm^2) for 24 hours. Western blots were performed for eNOS, PKCζ, and tubulin. (D) eNOS expression was analyzed by densitometry and normalized by setting static cells to 1.0. Data are mean ± SD of 3 experiments in triplicate. $**P < .05$.

Animal model and en face confocal analysis

All animal experiments were conducted in accordance with experimental protocols that were approved by the Institutional Animal Care and Use Committee at the University of Rochester. ApoE$^{-/-}$ mice on a C57BL/6J background were obtained from The Jackson Laboratory.

Immunofluorescence staining of mouse aortic ECs was performed as described previously.[30] Aortas of 12-week-old female ApoE$^{-/-}$ mice were perfused with PBS followed by 2% paraformaldehyde in PBS for 10 minutes. After fixation, the aortas were cut into small fragments and incubated in blocking buffer containing 2% bovine serum albumin and 0.1% Triton X-100 in PBS. Primary antibody incubations were performed overnight at 4°C. After washing the aortic segments 3 times, the secondary antibodies were added and incubated for 1 hour. For negative controls, nonimmune goat or rabbit immunoglobulin G was used in place of primary antibodies. After 3 washes, aortic specimens were opened, placed on a glass slide with the luminal side up, and then mounted for confocal microscopy (Olympus; FLUOVIEW300).

Statistical analysis

Data are shown as mean plus or minus SD for 3 to 4 separate experiments. Differences were analyzed by 1-way analysis of variance or Student *t* test. *P* values are expressed as less than .1 and less than .05. The latter was considered statistically significant.

Results

TNFα inhibits eNOS expression by a PKCζ-dependent pathway

To investigate the involvement of PKCζ activation in the TNFα-mediated inhibition of eNOS, we first treated BAECs with TNFα (0-10 ng/mL; 15 minutes), and PKCζ activity was measured by phosphorylation at Thr410 (p-PKCζ) by immunoblotting (Figure 1A-B). There was a significant 3-fold increase in PKCζ activity that was maximal at 5 ng/mL. TNFα treatment did not affect PKCζ expression in these cells (Figure 1A).

To study the effect of PKCζ activation on eNOS protein expression we used s-flow (12 dynes/cm^2; 24 hours) to stimulate eNOS expression. As shown in Figure 1C and D, s-flow increased eNOS expression by 1.3- plus or minus 0.09-fold ($N = 3$; $P < .05$). The addition of TNFα (10 ng/mL; 24 hours) had 2 significant effects on eNOS expression. First, there was a 55% decrease in expression (Figure 1D bars 1 vs 3), and second, the s-flow–mediated increase in eNOS expression (lanes 2 vs 1) was significantly inhibited by TNFα (lanes 4 vs 2). To determine whether this effect could be reversed by inhibiting PKCζ activity, we used the dominant-negative form of PKCζ (ATP binding site K to M mutant; DN-PKCζ). HUVECs were transduced with Ad.DN-PKCζ or adenoviral β-galactosidase (Ad.LacZ) and exposed to s-flow with or without TNFα. HUVECs transduced with Ad.LacZ expressed the same level of eNOS as sham-transfected cells (not shown) and Ad.DN-PKCζ (lanes 5 vs 1). Cells expressing Ad.DN-PKCζ exhibited an s-flow–mediated increase in eNOS expression (1.3-fold ± 0.1-fold; $N = 3$; $P < .05$) that did not differ from control Ad.LacZ-expressing cells (Figure 1C-D lanes 6 vs 2). More importantly, Ad.DN-PKCζ transduction significantly reduced the TNFα-mediated inhibition of eNOS expression in HUVECs exposed to s-flow (43% increase; Figure 1C lanes 8 vs 4). These data show that eNOS expression induced by s-flow is negatively regulated by PKCζ activity.

Methods

Antibodies, small interfering RNA, adenovirus, and reagents

Antibodies against ERK5 and p-PKCζ were purchased from Cell Signaling; anti-Flag and anti-tubulin from Sigma-Aldrich; anti-PKCζ, anti–hemagglutinin A (HA) and, anti–VP-16 from Santa Cruz Biotechnology Inc (CA); and anti-eNOS and anti– platelet endothelial cell adhesion molecule 1 (PECAM-1) from BD Transduction Laboratories. Peroxidase-conjugated goat anti–mouse and anti–rabbit antibodies were obtained from GE Healthcare. Alexa Fluor 488– or 546–conjugated goat anti–rabbit and anti–rat antibodies were purchased from Molecular Probes. The predesigned and prevalidated human-specific PKCζ small interfering RNA (siRNA; ON-TARGET plus SMART pool PKCζ siRNA; L-003526-00-00) and control siRNA were from Dharmacon RNA Technologies. Adenovirus that drives expression of a dominant-negative form of PKCζ (Ad.PKCζ-DN, ADV-112) was purchased from Cell Biolabs. TNFα was purchased from Roche Applied Science, and active recombinant human PKCζ was obtained from Stressgen Biotechnologies.

Plasmid construction

Mouse ERK5 and the constitutively active form of MEK5α (CA-MEK5α) were cloned as described previously.[26] PKCζ wild-type (WT) and catalytic domain (CATζ) constructs were kind gifts from Dr Jae-Won Soh (Columbia University), and eNOS promoter was a gift from Dr David Gardner (University of California, San Francisco). The reporter gene encoding KLF2 promoter (−924 to +14) was a gift from Dr Jerry Lingrel (University of Cincinnati). Gal4-ERK5 and VP16-ERK5 were created by inserting the mouse ERK5 isolated from pcDNA3.1-ERK5 into *Bam*H1 and *Not*1 sites of the pBIND and pACT vectors, respectively. Single mutations of ERK5 were created with the QuikChange site-directed mutagenesis kit (Stratagene). All constructs were verified by DNA sequencing.

Cell culture and transfection

Human umbilical vein endothelial cells (HUVECs) were obtained from collagenase-digested umbilical veins and collected in M200 medium supplemented with low serum growth supplement (Cascade Biologic), 5% fetal calf serum (GIBCO), 50 U/mL penicillin, and 50 μg/mL streptomycin. Bovine aortic ECs (BAECs) were cultured in M199 medium (GIBCO) supplemented with 10% fetal clone III (Hyclone), minimal essential medium (MEM)–amino acids, 50 U/mL penicillin, and 50 μg/mL streptomycin. HUVECs as well as BAECs were cultured on 2% gelatin precoated dishes. Chinese hamster ovary cells were cultured in F12 medium (GIBCO) supplemented with 10% fetal calf serum (GIBCO), 50 U/mL penicillin, and 50 μg/mL streptomycin. For transient expression experiments, 80% confluent cells were transfected with Opti-MEM and Lipofectamine 2000 (Invitrogen) as previously described.[27] Three hours after transfection, Opti-MEM was replaced with complete media, and cells were treated with TNFα 6 hours later.

For siRNA-driven depletion of PKCζ, HUVECs were transiently transfected with 40nM PKCζ or control siRNA with the use of Lipofectamine 2000 reagent. The cells were harvested 36 hours after siRNA transfection. For adenoviral infection, HUVECs were transduced with 50 multiplicity of infection of adenovirus expressing a dominant-negative form of PKCζ (Ad.PKCζ-DN)[28] and used 16 hours later.

Mammalian 1- or 2-hybrid analysis and transfection of cells

HUVECs were plated in 12-well plates at 5×10^4 cells/well. For mammalian one-hybrid analysis of transcriptional activity, cells were transfected in Opti-MEM with a Lipofectamine 2000 mixture containing pG5-luc vector, pBIND-ERK5, and pcDNA3 with or without pcDNA3-CA-MEKα. After 3 hours, cells were washed, and fresh medium supplemented with 10% fetal calf serum was added. Cells were treated 8 hours after transfection. For the mammalian 2-hybrid assay, cells were transfected in Opti-MEM with a Lipofectamine mixture containing the pG5-luc vector and various pBIND and pACT plasmids (Promega). Three hours later, Opti-MEM was replaced with complete medium, and cells were incubated overnight, washed twice with phosphate-buffered saline, and lysed in Passive Lysis Buffer (E194A; Promega). Luciferase assays were done with the Luciferase Assay system (E1501; Promega). Luciferase activity was normalized to β-galactosidase activity to correct for differences in transfection efficiency.

eNOS and KLF2 promoter activity

HUVECs were transiently cotransfected with human eNOS promoter (−1197) or KLF2 promoter (−924 to +14) and β-galactosidase with the use of Lipofectamine 2000. Luciferase activity was measured as above.

Steady laminar flow protocol

Confluent cells cultured in 100-mm dishes were exposed to s-flow (shear stress = 12 dyn/cm^2) with the use of a cone and plate type of flow apparatus placed in a humidified 5% CO_2 incubator at 37°C for 24 hours.

Western blot analysis and immunoprecipitation

Cells were harvested and lysed in RIPA buffer (5mM/L HEPES [N-2-hydroxyethylpiperazine;N′-2-ethanesulfonic acid], 10mM/L EDTA [ethylenediaminetetraacetic acid], 150mM/L NaCl, 1% NP-40, 0.5% sodium deoxycholate, 0.1% sodium dodecyl sulfate [SDS], pH 7.4) supplemented with the protease inhibitor cocktail.[29] Protein concentration was determined by Bradford assay (Bio-Rad), and cell lysates were subjected to SDS–polyacrylamide gel electrophoresis (PAGE). Proteins were then transferred onto nitrocellulose membranes, and the membranes were subsequently blocked with 5% nonfat dry milk in phosphate-buffered saline (PBS)/0.1% Tween20 for 1 hour. After being washed 3 times with PBS/0.1% Tween20, the blots were incubated overnight at 4°C with appropriate primary antibodies. Then, the membranes were incubated with peroxidase-conjugated secondary antibodies for 1 hour. Signals were visualized with the use of the enhanced chemiluminescence Western blotting detection system (Amersham Biosciences). Images were acquired with a Gel Doc System (Gel Doc 2000; Bio-Rad), and a densitometric analysis of membranes was performed using the Bio-Rad software. For the immunoprecipitation analysis, clarified supernatants (400 μg of total protein) were incubated with anti-Flag or anti-ERK5 at 4°C overnight. Lysates were then mixed with 50 μL of protein A/G agarose beads and incubated for 2 hours at 4°C. Immune complexes were collected by centrifugation (3000*g* for 2 minutes) and washed 4 times with the RIPA buffer, and then bound proteins were released in 2× SDS gel sample buffer. Then, the immunoprecipitates were subjected to SDS-PAGE and Western blot analysis.

In vitro phosphorylation of ERK5 by activated PKCζ

Glutathione-*S*-transferase (GST)–ERK5–truncated mutant proteins were expressed in *Escherichia coli*, purified with glutathione-Sepharose 4B as described (Pharmacia Biotech Inc), and used in in vitro kinase assays by activated PKCζ as described previously.[26] Briefly, each GST-ERK5 fragment (3 μg) was incubated for 30 minutes at 30°C in a reaction mixture (40 μL) containing 15 μmol/L adenosine triphosphate (ATP), 10mmol/L $MgCl_2$, 10mmol/L $MnCl_2$, 3 μCi (0.111 Bq) of [γ-^{32}P]ATP, and 10 ng of active recombinant human PKCζ. The reaction was terminated by adding 6 μL of 6× electrophoresis sample buffer and boiling for 5 minutes. Samples were analyzed on 10% SDS-PAGE, followed by autoradiography.

Real-time quantitative polymerase chain reaction analysis of eNOS and KLF2

Total RNA was isolated with the use of the TRIazol reagent (Invitrogen) and reverse transcription was conducted with the use of TaqMan reverse transcription reagents (Applied Biosystem) following the manufacturer's instruction. The relative quantities of specific mRNAs were obtained with the use of the comparative Ct method and were normalized to glyceraldehyde-3-phosphate dehydrogenase (Applied Biosystem).

PKCζ decreases eNOS protein stability via inhibitory phosphorylation of ERK5

Patrizia Nigro,[1] Jun-ichi Abe,[1] Chang-Hoon Woo,[2] Kimio Satoh,[3] Carolyn McClain,[1] Michael R. O'Dell,[1] Hakjoo Lee,[1] Jae-Hyang Lim,[4] Jian-dong Li,[4] Kyung-Sun Heo,[1] Keigi Fujiwara,[1] and Bradford C. Berk[1]

[1]Aab Cardiovascular Research Institute and Department of Medicine, University of Rochester Medical Center, NY; [2]Department of Pharmacology, College of Medicine, Yeungnam University, Daegu, Korea; [3]Department of Cardiovascular Medicine, Tohoku University Graduate School of Medicine, Sendai, Japan; and [4]Department of Microbiology and Immunology, University of Rochester Medical Center, NY

PKCζ has emerged as a pathologic mediator of endothelial cell dysfunction, based on its essential role in tumor necrosis factor α (TNFα)–mediated inflammation. In contrast, extracellular signal–regulated kinase 5 (ERK5) function is required for endothelial cell homeostasis as shown by activation of Krüppel-like factor 2 (KLF2), increased endothelial nitric-oxide synthase (eNOS) expression, and inhibition of apoptosis. We hypothesized that protein kinase C ζ (PKCζ) activation by TNFα would inhibit the ERK5/KLF2/eNOS pathway. TNFα inhibited the steady laminar flow–induced eNOS expression, and this effect was reversed by the dominant-negative form of PKCζ (Ad.DN-PKCζ). In addition, ERK5 function was inhibited by either TNFα or the transfection of the catalytic domain of PKCζ. This inhibition was reversed by PKCζ small interfering RNA. PKCζ was found to bind to ERK5 under basal conditions with co-immunoprecipitation and the mammalian 2-hybrid assay. Furthermore, PKCζ phosphorylates ERK5, and mutation analysis showed that the preferred site is S486. Most importantly, we found that the predominant effect of TNFα stimulation of PKCζ was to decrease eNOS protein stability that was recapitulated by transfecting Ad.ERK5S486A mutant. Finally, aortic en face analysis of ERK5/PKCζ activity showed high PKCζ and ERK5 staining in the athero-prone region. Taken together our results show that PKCζ binds and phosphorylates ERK5, thereby decreasing eNOS protein stability and contributing to early events of atherosclerosis. (*Blood*. 2010;116(11): 1971-1979)

Introduction

Endothelial nitric-oxide synthase (eNOS) is a key enzyme involved in the regulation of vascular function, and the altered activity and expression of this enzyme has been shown to contribute to atherosclerosis.[1-4] It has been reported that eNOS is regulated at the transcriptional, posttranscriptional, and posttranslational levels.[5,6] For example, tumor necrosis factor α (TNFα) has been shown to inhibit eNOS expression by down-regulating both transcriptional and posttranscriptional processes.[7-9]

Inflammation plays a central role in the pathogenesis of atherosclerosis.[10-13] TNFα, in addition to regulating eNOS expression, is a mediator of inflammation, and protein kinase C ζ (PKCζ) is a key enzyme for the TNFα-mediated inflammation. When endothelial cells (ECs) are stimulated by TNFα, PKCζ is activated and promotes monocyte adhesion by increased nuclear factor-κB–dependent intercellular adhesion molecule 1 expression.[14,15] In addition, we found that PKCζ activity was required for TNFα-mediated activation of c-Jun N-terminal kinase and caspase-3 in ECs,[16] events that cause endothelial dysfunction. Interestingly, increased PKCζ phosphorylation (ie, active form of the enzyme) was found in ECs located in the athero-susceptible region of porcine aorta.[17] Together, these observations suggest an important role of PKCζ in the process of atherogenesis by up-regulating inflammatory pathways in ECs.

A distinctive characteristic of PKCζ is the presence at the N-terminus of a novel protein-protein interaction module, termed PB1. The PB1 domain is named after the prototypical domain found in Phox and Bem1p, which mediate polar-heterodimeric interactions.[18] This domain is also present in the mitogen extracellular-signal-regulated kinase kinase 5 (MEK5), the upstream activator of the extracellular signal-regulated kinase 5 (ERK5), suggesting that there may be a cross talk between the PKCζ atherogenic and the MEK5-ERK5-KLF2 (Krüppel-like factor 2) atheroprotective signaling pathways. This latter pathway is activated by steady laminar flow (s-flow) and inhibits atherosclerosis.[19,20]

The atheroprotective effects of s-flow are well known. For example, we have earlier reported that s-flow potently activates ERK5[21] and that this s-flow–mediated ERK5 activation induces the expression of KLF2, a recently identified transcriptional activator of eNOS and an inhibitor of EC inflammation.[22,23] Furthermore, we have shown that peroxisome proliferator activated receptor γ1 is activated by s-flow by way of ERK5 activation and contributes to the overall anti-inflammatory and athero-protective effects of flow.[24] In addition to its kinase activity, ERK5 acts as a transcriptional activator. The C-terminus region of ERK5 has 2 transactivation domains, one of them (aa684-806) is constitutively active. Importantly, proatherogenic stimuli inhibit ERK5 activity, in part by stimulating SUMOylation at Lys6 and Lys22, which decreases flow-mediated KLF2 promoter activity and eNOS expression.[25]

The mechanism by which TNFα decreases eNOS expression in ECs is not fully elucidated. Here, we study the involvement of PKCζ and the MEK5/ERK5 pathway in the TNFα-induced down-regulation of eNOS expression in ECs and in the initiation of atherosclerosis.

Submitted February 8, 2010; accepted May 23, 2010. Prepublished online as *Blood* First Edition paper, June 10, 2010; DOI 10.1182/blood-2010-02-269134.

The online version of this article contains a data supplement.

The publication costs of this article were defrayed in part by page charge payment. Therefore, and solely to indicate this fact, this article is hereby marked "advertisement" in accordance with 18 USC section 1734.

Cardiovascular Research (2009) 81, 226–234
doi:10.1093/cvr/cvn244

Statin ameliorates hypoxia-induced pulmonary hypertension associated with down-regulated stromal cell-derived factor-1

Kimio Satoh[1], Yoshihiro Fukumoto[1]*, Makoto Nakano[1], Koichiro Sugimura[1], Jun Nawata[1], Jun Demachi[1], Akihiko Karibe[1], Yutaka Kagaya[1], Naoto Ishii[2], Kazuo Sugamura[2], and Hiroaki Shimokawa[1,3]

[1]*Department of Cardiovascular Medicine, Tohoku University Graduate School of Medicine, 1-1 Seiryo-machi, Aoba-ku, Sendai 980-8574, Japan;* [2]*Department of Microbiology and Immunology, Tohoku University Graduate School of Medicine, Sendai, Japan and* [3]*Technology Agency, CREST, Tokyo, Japan*

Received 21 July 2008; revised 28 August 2008; accepted 4 September 2008; online publish-ahead-of-print 8 September 2008

Time for primary review: 29 days

KEYWORDS
Statin;
Pulmonary hypertension;
Hypoxia;
Myofibroblast;
Progenitors

Aims Mobilization of stem cells/progenitors is regulated by the interaction between stromal cell-derived factor-1 (SDF-1) and its ligand, CXC chemokine receptor 4 (CXCR4). Statins have been suggested to ameliorate pulmonary arterial hypertension (PAH); however, the mechanisms involved, especially their effects on progenitors, are largely unknown. Therefore, we examined whether pravastatin ameliorates hypoxia-induced PAH in mice, and if so, which type of progenitors and what mechanism(s) are involved.

Methods and results Chronic hypoxia (10% O_2 for 5 weeks) increased the plasma levels of SDF-1 and mobilization of $CXCR4^+$/vascular endothelial growth factor receptor (VEGFR)2^+/c-kit^+ cells from bone marrow (BM) to pulmonary artery adventitia in Balb/c mice *in vivo*, both of which were significantly suppressed by simultaneous oral treatment with pravastatin (2 mg/kg/day). Furthermore, *in vitro* experiments demonstrated that hypoxia enhances differentiation of $VEGFR2^+$/c-kit^+ cells into α-smooth muscle $actin^+$ cells. Importantly, pravastatin ameliorated hypoxia-induced PAH associated with a decrease in the number of BM-derived progenitors accumulating in the pulmonary artery adventitia. The expression of intercellular adhesion molecule-1 (ICAM-1) and its ligand, CD18 (β2-integrin), were enhanced by hypoxia and were again suppressed by pravastatin.

Conclusions These results suggest that pravastatin ameliorates hypoxia-induced PAH through suppression of SDF-1/CXCR4 and ICAM-1/CD18 pathways with a resultant reduction in the mobilization and homing of BM-derived progenitor cells.

1. Introduction

Recent reports demonstrated that circulating endothelial progenitor cells (EPCs) promote endothelial repair, which is enhanced by 3-hydroxy-3-methylglutaryl-coenzyme A reductase inhibitors (statins).[1–3] Moreover, the number of circulating EPCs correlates with endothelial function and the degree of coronary artery disease in humans.[4] Accumulating evidence suggests that circulating EPCs are mobilized to the site of ischaemia by several humoral factors, such as vascular endothelial growth factor (VEGF), stromal cell-derived factor-1 (SDF-1), CD18, and intercellular adhesion molecule-1 (ICAM-1), contributing to the neovascularization.[1,5,6] Recently, it has also been reported that CXC chemokine receptor 4 (CXCR4), the receptor for SDF-1, plays an important role in the mobilization and recruitment of bone marrow (BM)-derived cells.[7] We have recently reported that EPCs are mobilized under hypoxic conditions and are incorporated into the pulmonary endothelium in pulmonary arterial hypertension (PAH) in mice.[8] Recent studies also demonstrated the therapeutic effects of EPC transplantation in animal models of PAH.[9,10] However, it remains to be examined whether EPCs also exert beneficial effects in patients with PAH, which is characterized by plexiform lesion composed of actively proliferating endothelial cells.[11]

It has been demonstrated that statins could prevent the development of PAH in animal models.[12–14] Although statins could mobilize EPCs,[15,16] long-term statin treatment has been reported to reduce the number of circulating EPCs in patients with coronary artery disease.[17] Therefore,

* Corresponding author. Tel: +81 22 717 7153; Fax: +81 22 717 7156.
E-mail address: fukumoto@cardio.med.tohoku.ac.jp

statins might have biphasic effects on mobilization of EPCs,[18] as well as other circulating progenitor cells, which have also been reported to exist and differentiate into α-smooth muscle actin (SMA)$^+$ cells in humans,[19,20] and may participate in the progression of atherosclerosis[21–23] and lung fibrosis.[24] Recent reports also showed the existence of circulating progenitors that exhibit fibroblast-like properties, migrate into the pulmonary vasculature, and promote adventitial remodelling as myofibroblasts (α-SMA-expressing fibroblasts) in hypoxia-induced PAH.[25–27] Indeed, the BM-derived progenitors could differentiate into α-SMA$^+$ cells in hypoxia-induced PAH in mice.[28] However, it largely remains unknown whether statins affect mobilization and recruitment of those progenitors.

In the present study, we thus examined whether pravastatin ameliorates hypoxia-induced PAH in mice, and if so, which type of progenitors and what mechanism(s) are involved.

2. Methods

All procedures were performed according to the protocols approved by the Institutional Committee for Use and Care of Laboratory Animals of Tohoku University and the Guide for Care and Use of Laboratory Animals published by the US National Institutes of Health (NIH publication 8523, revised 1985). The authors had full access to the data and take full responsibility for its integrity. All authors have read and agree to the article as written.

2.1 Animal preparation

In the present study, we used 16-week-old wild-type (WT, $n = 56$) mice of Balb/c background. ROSA26 (LacZ) mice that express β-galactosidase (β-gal) activity in all tissues[29] were purchased from Jackson Laboratory (Bar Harbor, ME, USA).

2.2 Hypoxia-induced pulmonary arterial hypertension model in mice and statin treatment

The present study is a preventive study in nature. Four weeks after the BM transplantation, β-gal-BM chimeric mice were randomized to receive either pravastatin (2 mg/kg/day) or vehicle by daily gavage, and then exposed to hypoxia (10% O_2, for *in vivo* experiment) for 5 weeks in a hypoxic chamber, as previously described.[8,12] As a control, chimeric mice were maintained in plastic cages in ambient air (21% O_2). After 5 weeks of chronic hypoxia, control and hypoxic mice were anaesthetized with intraperitoneal ketamine hydrochloride (60 mg/kg) and xylazine (8 mg/kg) ($n = 10$, respectively), and right ventricular systolic pressure (RVSP) was measured by percutaneous insertion into the right ventricle (RV) through the subxiphoid approach of a 25-gauge needle connected to a pressure transducer without the use of respirator nor opening the chests. To evaluate the extent of RV hypertrophy, the RV free wall and left ventricle (LV) plus septum (LV+S) were weighed separately.

2.3 *Ex vivo* culture of mononuclear cells

To confirm the differentiation capacity, isolated peripheral blood mononuclear cells (PBMCs) from hypoxic mice (10% O_2 for 7 days) were cultured on collagen I-coated chamber slides (BioCoat; Becton Dickinson, San Jose, USA) in Dulbecco's modified Eagle's medium (DMEM) supplemented with 10% foetal bovine serum (FBS), 100 U/mL penicillin, and 100 μg/mL streptomycin in hypoxic conditions (2% O_2, 5% CO_2, and 93% nitrogen, 33°C, for *in vitro* experiment). For immunohistological staining, monoclonal antibody to fluorescein isothiocyanate (FITC)-labelled α-SMA (1:400, Sigma, St Louis, USA) was used for primary antibody.

2.4 Fluorescence-activated cell sorter analysis

Fluorescence-activated cell sorter (FACS) analysis was performed as described previously.[8,9] To quantify the number of VEGFR2$^+$/c-kit$^+$ cells, we used phycoerythrin-labelled anti-mouse VEGFR2, FITC-labelled anti-mouse c-kit (eBioscience), and biotinylated anti-mouse lineage antibodies (Mac-1, Gr-1, B220, CD4, CD8, and Ter119) and APC-labelled streptavidin (BD PharMingen). Quantitative analysis was performed by FACS analysis (FACSCalibur; Becton Dickinson).

2.5 Cell sorting by fluorescence-activated cell sorter

BM cells were obtained from hypoxic mice, and BM mononuclear cells were isolated by density gradient centrifugation with Nycoprep Animal 1.077 (Axis-Shield). Lin$^-$ /VEGFR2$^+$/c-kit$^+$ cells were selected with a cell sorting system (FACSAria; Becton Dickinson Immunocytometry Systems).[30]

2.6 Bone marrow transplantation

BM transplantation was performed as described previously.[8] The chimeric rate was >95% by FACS analysis.

2.7 Immunofluorescence staining

Immunofluorescence staining was performed on 4% of paraformaldehyde-fixed frozen sections as previously described.[8] The primary antibodies used were FITC-labelled anti-β-gal (1:400; Abcam Ltd, Cambridge, UK), anti-mouse ICAM-1 (1:400; BD PharMingen), anti-mouse CD18 (1:400; BD PharMingen), Cy3-labelled anti-α-SMA (1:400; Sigma), anti-VEGFR2 (1:200; Santa Cruz), anti-CD31, biotinylated anti-c-kit, and biotinylated anti-CXCR4 (1:400; BD PharMingen, San Diego). As the secondary antibodies, Cy3- or Cy5-labelled antibodies were used (Jackson ImmunoResearch Laboratories). Vectashield mounting medium with DAPI (vector) was used to counterstain nuclei. Slides were viewed with a confocal fluorescence microscope (Fluoview FV1000, Olympus, Tokyo, Japan). As a negative control, species- and isotype-matched IgG were used in place of the primary antibody.

2.8 X-gal staining

To detect β-gal-positive cells, the lungs were perfusion-fixed with 0.5% glutaraldehyde (pH 7.2) at 4°C and the whole lungs were incubated at 37°C for 18 h in X-gal (5-bromo-4-chloro-3-indolyl β-D-galactopyranoside) solution as previously described.[29]

2.9 Plasma levels of stromal-derived factor-1

Plasma levels of SDF-1 were evaluated by ELISA with a mouse SDF-1 Quantikine kit (R&D) following the manufacture's protocol.

2.10 Statistical analysis

Quantitative results are expressed as means ± SD. Statistical analysis was performed with StatView (StatView 5.0, SAS Institute Inc., Cary, NC, USA). Comparisons of parameters among the three groups were made by one-way ANOVA and those between the two groups under different conditions by two-way ANOVA followed by Bonferroni *post hoc* test. A value of $P < 0.05$ was considered to be statistically significant.

3. Results

3.1 Mobilization of vascular endothelial growth factor receptor 2$^+$/c-kit$^+$ cells in hypoxia-induced pulmonary arterial hypertension in mice

To elucidate the role of circulating VEGFR2$^+$/c-kit$^+$ cells, we performed FACS analysis on PBMCs from the mice that were

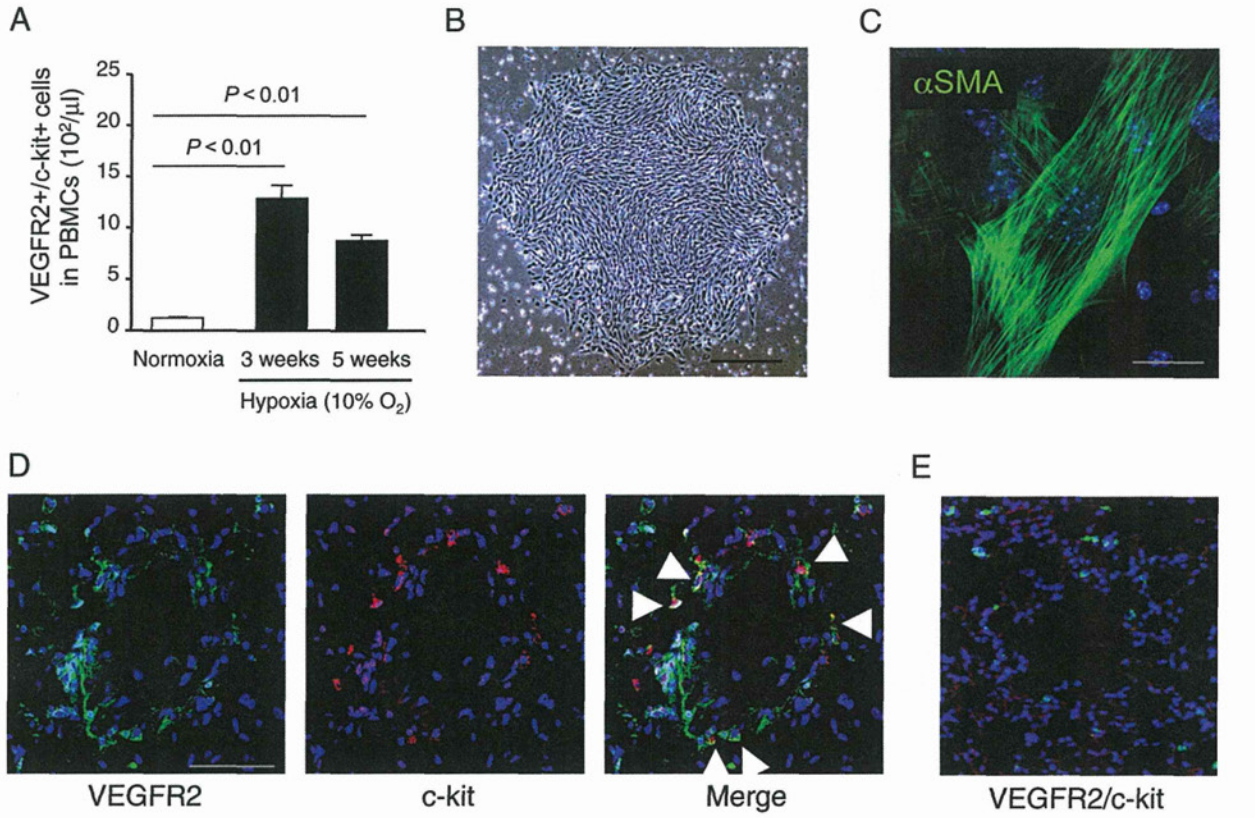

Figure 1 Vascular endothelial growth factor receptor (VEGFR)2^+/c-kit^+ cells to the adventitia of pulmonary arteries in hypoxia. (*A*) Fluorescence-activated cell sorter analysis indicated that hypoxia significantly increased the number of circulating VEGFR2^+/c-kit^+ cells at 3 and 5 weeks ($n = 6$ each). Results are expressed as means ± SD. (*B*) Colonies with a 'hill and valley' morphology after cultivation of peripheral blood mononuclear cells for 3 weeks under hypoxic conditions (2% O_2). Scale bar: 200 μm. (*C*) α-SMA immuno-positive cells in the colony. Scale bar: 10 μm. (*D,E*) VEGFR2^+/c-kit^+ cells in the adventitia of pulmonary arteries in mice with hypoxic condition (5 weeks) detected by immunostaining (*D*, arrows), but not in normoxic mice (*E*). Scale bar: 50 μm.

chronically exposed to hypoxia (10% O_2) for 5 weeks. Interestingly, the number of cells was significantly increased in hypoxic mice compared with that in normoxic mice at 3 and 5 weeks of hypoxia (*Figure 1A*). Moreover, cultivation of PBMCs from hypoxic mice revealed a colony formation (*Figure 1B*). Immunostaining revealed that these cells were positive for α-SMA (*Figure 1C*). Furthermore, VEGFR2^+/c-kit^+ cells were accumulated mainly at the adventitia of pulmonary arteries of chronically hypoxic mice (*Figure 1D*), whereas VEGFR2^+/c-kit^+ cells were not observed in normoxic condition (*Figure 1E*). These results suggest a crucial role of circulating VEGFR2^+/c-kit^+ cells in the pathogenesis of hypoxia-induced PAH.

3.2 Differentiation of vascular endothelial growth factor receptor 2^+/c-kit^+ cells into α-smooth muscle $actin^+$ cells

To elucidate the role of VEGFR2^+/c-kit^+ cells, we isolated VEGFR2^+/c-kit^+ cells from BM of Rosa26 mice by flow cytometry (*Figure 2A*) and cultured them on primary cultured stromal cell layers (derived from WT mice) under hypoxic conditions (2% O_2, 33°C) for 3 weeks (*Figure 2B*). Interestingly, these cells differentiated into α-SMA^+ cells after 3 weeks of culture (*Figure 2C*).

3.3 Pravastatin reduces the number of bone marrow-derived cells at the pulmonary artery adventitia

To elucidate the effects of pravastatin on the recruitment of the BM-derived cells and the development of pulmonary vascular remodelling, we used chimeric mice with β-gal-labelled BM. These chimeric mice were chronically exposed to hypoxia (10% O_2) for 5 weeks with or without simultaneous treatment with pravastatin (2 mg/kg/day). Microscopic observation revealed that the BM-derived (β-gal^+) cells migrated and accumulated to the adventitia of pulmonary arteries (*Figure 3A*) and that pravastatin significantly reduced the number of those cells (*Figure 3A* and *B*).

3.4 Pravastatin reduces mobilization of vascular endothelial growth factor receptor 2^+/c-kit^+ cells and ameliorates pulmonary arterial hypertension

It has been shown that the secretion of SDF-1 is controlled by hypoxia-induced factor-1α (HIF-1α), which have chemotactic power to mobilize the BM-derived progenitors.[31,32] We therefore assessed the plasma levels of SDF-1 in chronically hypoxic mice with or without pravastatin. Interestingly, plasma levels of SDF-1 were significantly increased in hypoxic mice, which was significantly reduced by pravastatin (*Figure 4A*). Moreover, immunostaining revealed that hypoxia enhanced the accumulation of $CXCR4^+$ cells in the lung (*Figure 4B*) and FACS analysis showed the hypoxia-induced increase in the number of circulating $CXCR4^+$/VEGFR2^+/c-kit^+ cells in peripheral blood (*Figure 4C*), both of which also were inhibited by pravastatin. Finally, we confirmed that pravastatin ameliorated PH in mice *in vivo*, as assessed by RVSP (*Figure 4D*) and RV hypertrophy (*Figure 4E*).

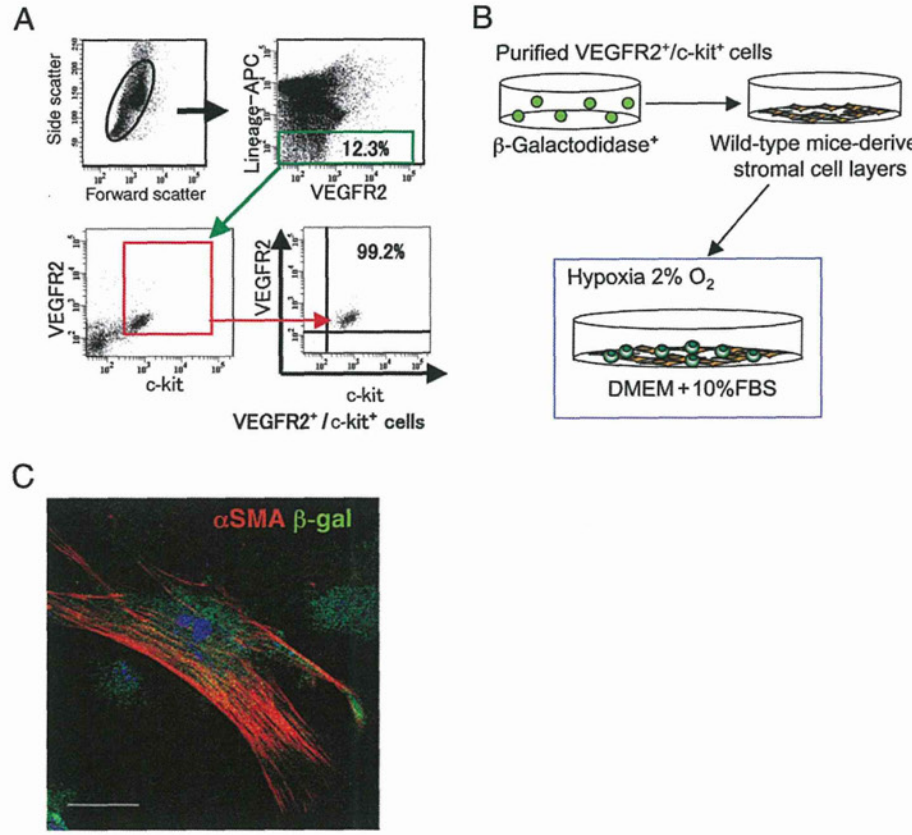

Figure 2 Differentiation of purified vascular endothelial growth factor receptor (VEGFR)2$^+$/c-kit$^+$ cells into α-smooth muscle actin (SMA)$^+$ cells under hypoxic conditions. (*A*) Purification from the bone marrow of ROSA26 mice by flow cytometry. (*B*) Cultivation on the irradiated stromal cell layers under hypoxic conditions for 3 weeks. (*C*) Differentiation of purified VEGFR2$^+$/c-kit$^+$ cells (β-galactosidase$^+$) into α-SMA$^+$ cells. Scale bar: 10 μm.

3.5 Pravastatin reduces accumulation of bone marrow-derived cells by suppressing ICAM-1 expression

It has been implicated that the interaction between ICAM-1 and its ligand, CD18, is crucial for the recruitment of the BM-derived progenitors.[33] We therefore assessed ICAM-1 expression in the hypoxic lung, the number of BM-derived cells, and their CD18 expression. Interestingly, hypoxia enhanced the expression of ICAM-1 in the lung, which was again suppressed by pravastatin (*Figure 5A*). Moreover, the BM-derived CD18$^+$ cells accumulated into the pulmonary artery adventitia in hypoxic lung, which was again reduced by pravastatin (*Figure 5A* and *B*).

4. Discussion

The novel findings of the present study were that: (i) chronic hypoxia significantly mobilized VEGFR2$^+$/c-kit$^+$ cells that accumulated into the pulmonary artery adventitia *in vivo* and differentiated into α-SMA$^+$ cells *in vitro* and (ii) pravastatin reduced the plasma levels of SDF-1, mobilization of CXCR4$^+$/VEGFR2$^+$/c-kit$^+$ cells, and the expression of ICAM-1 in the lung, resulting in the reduced accumulation of BM-derived progenitors and amelioration of PAH. The present findings are summarized in *Figure 6*. To the best of our knowledge, this is the first study that demonstrates the therapeutic effects of a statin for PAH in the cutting edge of circulating progenitors.

4.1 Circulating progenitors and pulmonary arterial hypertension

We have recently demonstrated that circulating progenitors are incorporated into the pulmonary endothelium and that mobilization and homing of progenitors are important in the pulmonary vascular remodelling as they exert beneficial effects in hypoxia-induced PAH in mice.[8] In the present study, circulating mononuclear cells isolated from mice chronically exposed to hypoxia differentiated into α-SMA$^+$ cells *in vitro*. Consistent with our finding, a recent report demonstrated that circulating c-kit$^+$ progenitor cells are involved in vessel wall thickening in hypoxia-induced PAH in calves.[25] Moreover, it has been shown that BM-derived cells differentiate into α-SMA$^+$ cells in pulmonary arteries in hypoxia-induced PAH in mice.[28] It has also been demonstrated that circulating progenitors are heterogeneous and that haematopoietic stem cell-derived progenitors contribute to neoangiogenesis through adventitial infiltration, without any contributions to pulmonary endothelium in PAH animal models.[34,35] Therefore, the BM-derived circulating progenitors may play a crucial role in the development of hypoxia-induced pulmonary vascular remodelling.

In the present study, we were also able to demonstrate the significant mobilization and accumulation of VEGFR2$^+$/c-kit$^+$ cells at the pulmonary artery adventitia *in vivo* and their differentiation into α-SMA$^+$ cells *ex vivo*. Recent reports demonstrated that α-SMA$^+$ cells at the pulmonary artery adventitia can be derived from circulating

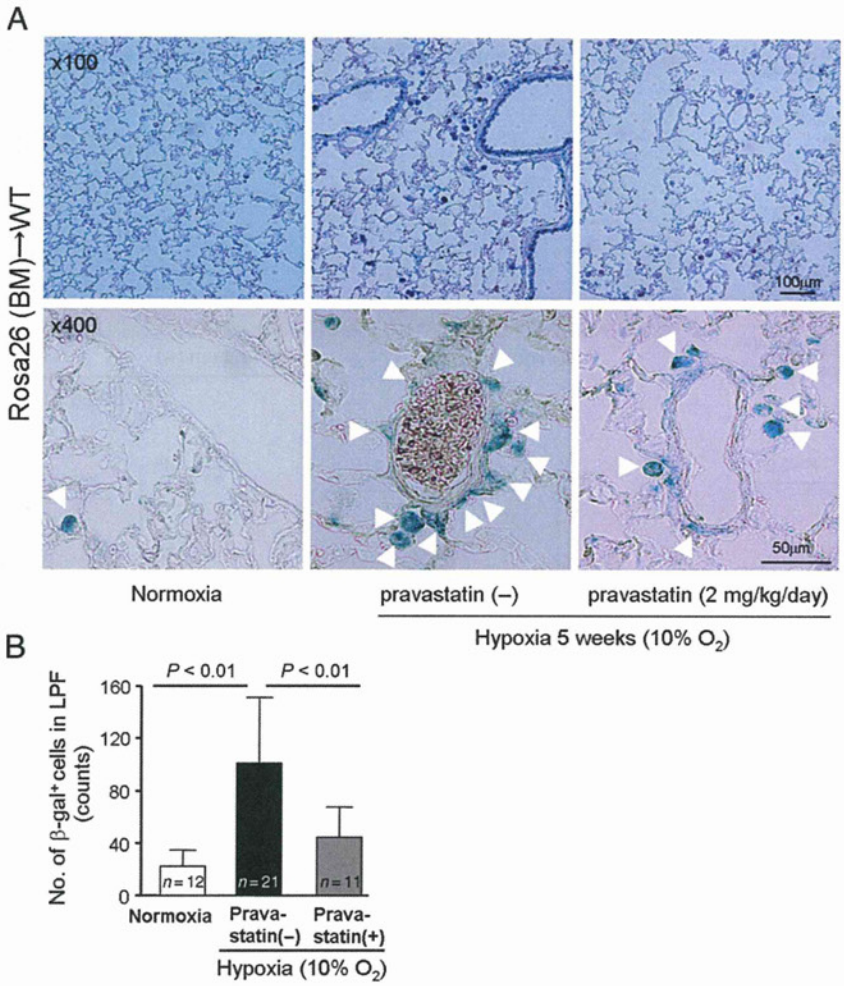

Figure 3 Bone marrow (BM)-derived cells in the adventitia of pulmonary arteries of chimeric mice. (*A*) X-gal staining showed that β-galactosidase (β-gal)$^+$ BM-derived cells were increased by hypoxia and accumulated to the pulmonary artery adventitia (arrowheads) in hypoxic mice, while the number of BM-derived cells was reduced by pravastatin (arrowheads). (*B*) The number of β-gal$^+$ cells was significantly increased in the hypoxic lung, which was significantly suppressed by pravastatin. Results are expressed as means ± SD. Normoxia, normoxic mice; hypoxia, mice exposed to 5 weeks of hypoxia (10% O_2) with or without pravastatin (2 mg/kg/day). LPF, low-power field (×200).

progenitors and have a potential to migrate and incorporate into the media and contribute to medial thickening.[26,36] These reports and our present findings suggest the existence of circulating progenitor cells for α-SMA$^+$ cells and their crucial roles in the pathogenesis of pulmonary vascular remodelling in hypoxia-induced PAH.

4.2 Statins and pulmonary arterial hypertension

It has been recently demonstrated that statins induce apoptosis of neointimal smooth muscle cells[37] and ameliorate monocrotaline-induced PAH in rats.[12] Statins have also been shown to prevent pulmonary artery muscularization and progression of PAH by protecting expression and activity of endothelial nitric oxide synthase (eNOS) at post-transcriptional level in hypoxia-induced PAH in rats.[14,38] Although the mechanisms underlying the beneficial effects of statins on PAH are not fully elucidated, these studies suggest that statins may improve endothelial function, at least in part, through NO-dependent mechanisms.[12,14,38] On the other hand, it also has been shown that statins mobilize progenitors and activate their function through up-regulation of eNOS.[15,16,18] However, in the present study, the number of circulating progenitors assessed by FACS analysis was significantly reduced by pravastatin in hypoxic mice. Therefore, the effect of statins on mobilization of progenitors under hypoxic conditions may have a complex mechanism (*Figure 6*).

Recently, it has been shown that SDF-1 plays a crucial role to mobilize and recruit BM-derived CXCR4$^+$ proangiogenic cells to the ischaemic tissue.[31] Moreover, it has been shown that the activated perivascular myofibroblasts produce abundant SDF-1, which plays a crucial role in the recruitment of BM-derived cells to the perivascular area.[32] Again, recruited CXCR4$^+$ cells secret angiogenic cytokines and promote the proliferation and differentiation of resident cells in vascular walls.[31,32] In the present study, we demonstrated that pravastatin significantly reduced the plasma levels of SDF-1, which could explain, at least in part, for the reduced mobilization of progenitors by statin. Pravastatin also suppressed the expression of ICAM-1 that is important for homing of BM-derived cells to the ischaemic tissue.[33] Taken together, we were able to demonstrate that pravastatin significantly reduces mobilization and homing of

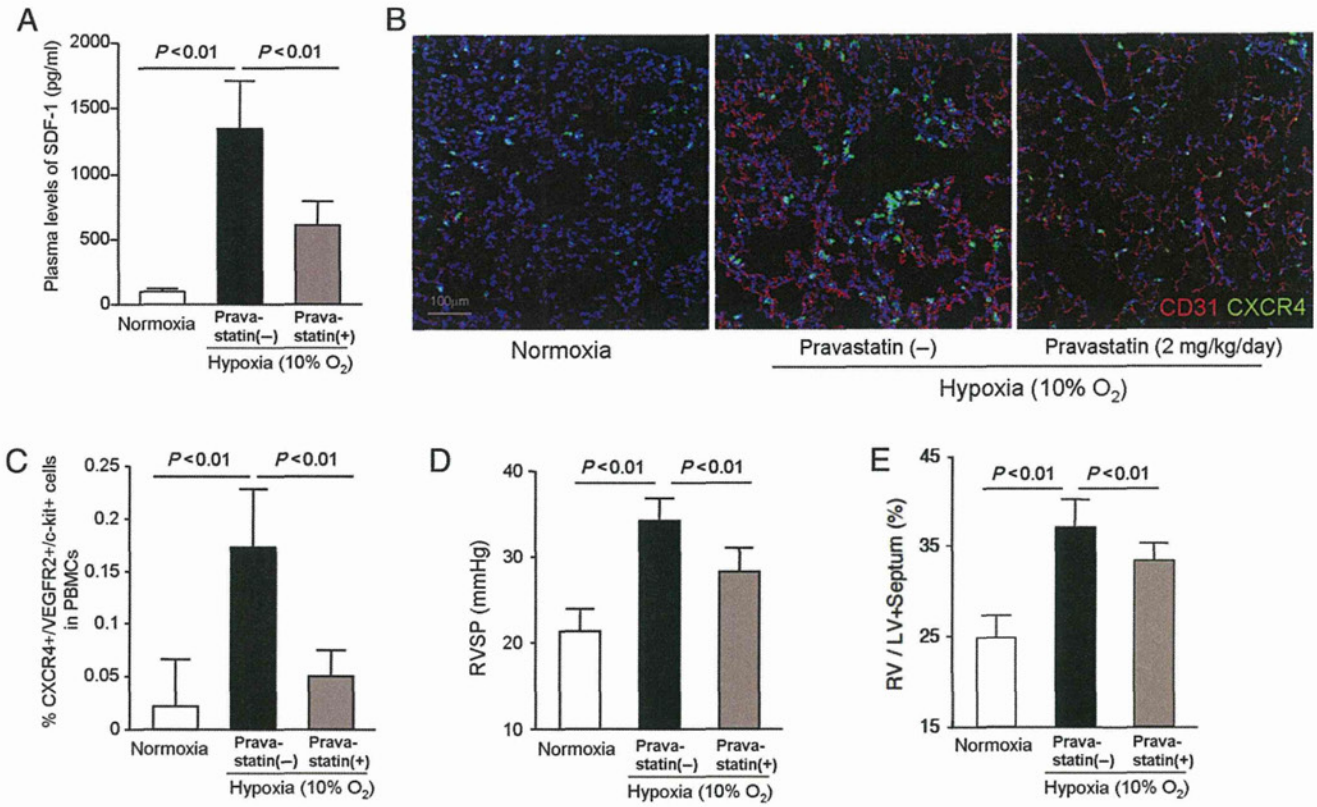

Figure 4 Reduction in plasma levels of stromal cell-derived factor (SDF)-1, mobilization of CXC chemokine receptor (CXCR)4$^+$/vascular endothelial growth factor receptor (VEGFR)2$^+$/c-kit$^+$cells, and ameliorated pulmonary arterial hypertension (PAH) by pravastatin. (*A*) Plasma levels of SDF-1 in hypoxic mice with or without pravastatin ($n = 11$ each). (*B*) Immunostaining of lung sections with CXCR4 (green signals) and CD31 (red signals) revealed the accumulation of CXCR4$^+$ cells in hypoxic lung, which was reduced by pravastatin. (*C*) Hypoxia significantly increased the number of CXCR4$^+$/VEGFR2$^+$/c-kit$^+$ cells in the peripheral blood, which was significantly suppressed by pravastatin ($n = 5$ each). (*D,E*) Pravastatin suppressed the development of hypoxia-induced PAH, as assessed by RV systolic pressure (RVSP) (*D*) and RV hypertrophy (*E*) in mice ($n = 10$ each). The extent of RV hypertrophy is expressed as a ratio of RV mass to LV plus septal mass (RV/LV + Septum). Results are expressed as means ± SD.

BM-derived cells, resulting in the inhibition of hypoxia-induced pulmonary artery remodelling and PAH (*Figure 6*).

4.3 Limitations of the study

There are several limitations should be mentioned for the present study.

First, hypoxia-induced PAH model may not fully represent the primary PAH in humans because this model shows considerably high plasma levels of cytokines/chemokines.[39] It has been shown that hypoxia increases the expression of SDF-1 through HIF-1-dependent mechanisms.[40] Consistently, in the present study, plasma level of SDF-1 was significantly increased in WT mice in response to hypoxia. Additionally, pravastatin significantly reduced the plasma levels of SDF-1 and ameliorated hypoxia-induced PAH, although the precise mechanism remains to be elucidated in future studies. On the other hand, blockade of SDF-1 by specific antibody has been shown to reduce neointimal formation in ApoE$^{-/-}$ mice by regulating neointimal smooth muscle content.[41] Taken together, it is possible that SDF-1 also plays a crucial role in the development of pulmonary vascular remodelling in PH.

Second, the role of EPCs in the development of PAH in humans remains to be elucidated. It was demonstrated that the number of circulating endothelial cells was significantly increased in patients with PAH.[11] The number of circulating EPCs is regulated not only by their recruitment or mobilization but also by their activity and consumption in the peripheral vasculature.[1–4] Therefore, when considering a therapy focusing on BM-derived progenitors, it would be important to evaluate their mobilization and homing as well as the character of each progenitor.

Third, it remains to be examined whether statins could ameliorate PH in humans through down-regulation of SDF-1. However, this important issue is beyond the scope of the present study, and we would like to address this issue in future studies.

Fourth, in the present study, we have demonstrated that the number of progenitor cells is decreased by co-treatment with pravastatin in which finding is different from that in atherosclerotic model.[42] Thus, future studies are needed to determine the role of progenitor cells, especially at the adventitia.

Fifth, the present study is a preventive study in nature. Because oxidative stress contributes to the initiation and the development of hypoxia-induced tissue injury and PAH, statins may be expected to reduce initial oxidative and subsequent events that lead to PAH. In this regard, statins have direct antioxidant effects: inhibit NAD[P]H activity and up-regulate the activity of antioxidant enzymes, such as catalase and paraoxonase, and also reduce circulating oxidized low-density lipoprotein (ox-LDL), inhibit ox-LDL uptake by macrophages, and reduce circulating markers of oxidation, such as F2-isoprostane and nitrotyrosine. Thus, it remains to be examined in future studies whether

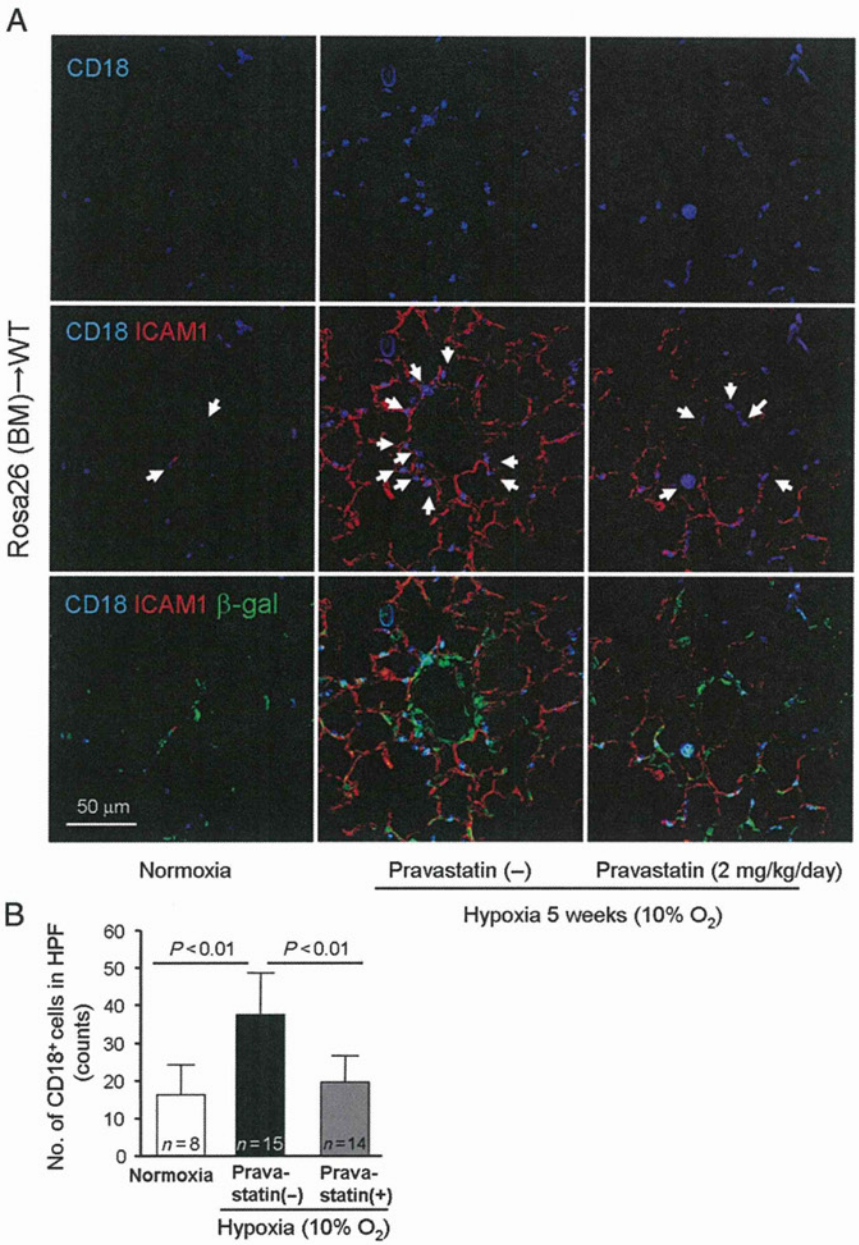

Figure 5 Bone marrow (BM)-derived cells in the adventitia of pulmonary arteries of chimeric mice through the suppression of intercellular adhesion molecule (ICAM)-1/CD18 interaction. (*A*) Immunostaining revealed that the expression of ICAM-1 (red signals) is enhanced in the lung and $CD18^+$ cells (blue signals) are accumulated to the pulmonary artery adventitia (arrowheads) in hypoxic mice. Pravastatin reduced the number of $CD18^+$/β-galactosidase $(\beta\text{-gal})^+$ cells that accumulated to the pulmonary artery adventitia (CD18/ICAM-1/β-gal). β-gal is expressed as green signals. (*B*) The number of $CD18^+$ cells was significantly increased in hypoxic lung, which was significantly suppressed by pravastatin. Results are expressed as means ± SD. Normoxia, normoxic mice; hypoxia, mice exposed to 5 weeks of hypoxia (10% O_2) with or without pravastatin (2 mg/kg/day). HPF, high-power field (×400).

statins exerts beneficial effects in animals with fully developed disease.

4.4 Clinical implications

We have previously demonstrated that statins alter smooth muscle cell accumulation and collagen content in established atheroma in rabbits.[43] It has recently been demonstrated that statins ameliorate congestive heart failure,[44] ischaemia/reperfusion injury,[45] and PAH[46] in humans. In the present study, we were able to demonstrate that pravastatin ameliorates PAH in mice associated with a marked reduction in the number of BM-derived progenitors at the pulmonary artery adventitia. Indeed, it was shown that *in vivo* depletion of circulating progenitors for $\alpha\text{-SMA}^+$ cells resulted in marked attenuation of hypoxia-induced pulmonary vascular remodelling, such as adventitial thickening, perivascular fibrosis, and myofibroblast accumulation.[27] Therefore, modulation of mobilization and homing of BM-derived cells by statins could be a new therapeutic strategy for the treatment of PAH in humans.

Funding

This work was supported in part by the grants-in-aid (Nos. 15256003, 16209027, 16659192, 18659218) from the Japanese Ministry of Education, Culture, Sports, Science, and Technology, Tokyo, Japan, the Japanese Ministry of Health, Labor, and Welfare, Tokyo, Japan; the

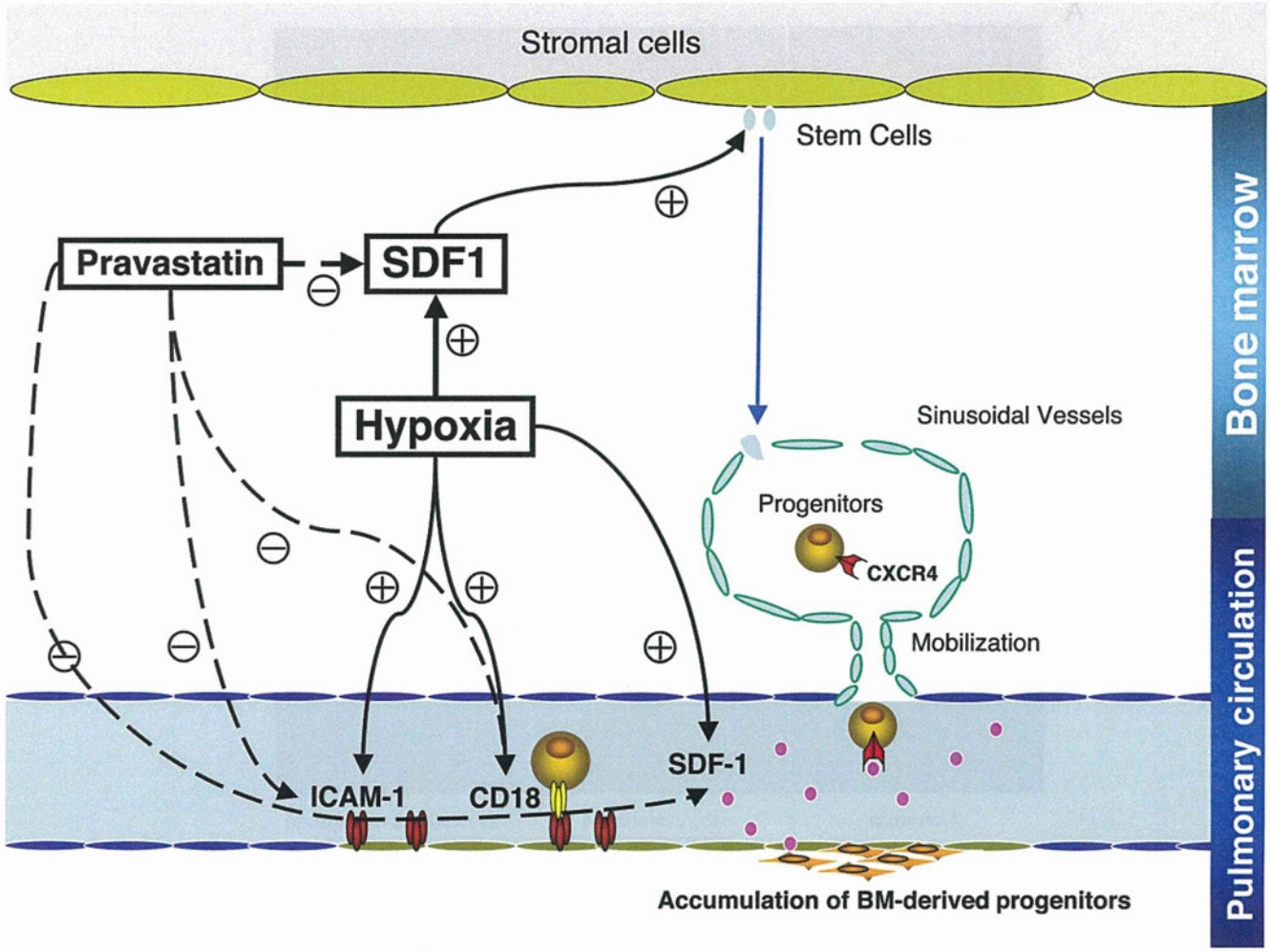

Figure 6 Summary of the present study. Stromal cell-derived factor (SDF)-1 mediates the mobilization and chemotaxis of bone marrow (BM)-derived progenitors in response to hypoxia. During the development of hypoxia-induced pulmonary vascular remodelling, pravastatin reduces the plasma levels of SDF-1 and the expression of intercellular adhesion molecule (ICAM)-1 in the lung, resulting in the reduced number of BM-derived progenitors in the adventitia and the amelioration of pulmonary arterial hypertension. Solid line, proven mechanism; dashed line, proposed mechanism; plus, stimulation; minus, inhibition.

Japan Foundation of Cardiovascular Research, Tokyo, Japan, the Program for Promotion of Fundamental Studies in Health Sciences of the Organization for Pharmaceutical Safety and Research of Japan; and Technology Agency, CREST, Tokyo, Japan.

Conflict of interest: none declared.

References

1. Asahara T, Murohara T, Sullivan A, Silver M, van der Zee R, Li T *et al.* Isolation of putative progenitor endothelial cells for angiogenesis. *Science* 1997;**275**:964–967.
2. Walter DH, Rittig K, Bahlmann FH, Kirchmair R, Silver M, Murayama T *et al.* Statin therapy accelerates reendothelialization: a novel effect involving mobilization and incorporation of bone marrow-derived endothelial progenitor cells. *Circulation* 2002;**105**:3017–3024.
3. Urbich C, Knau A, Fichtlscherer S, Walter DH, Bruhl T, Potente M *et al.* FOXO-dependent expression of the proapoptotic protein Bim: pivotal role for apoptosis signaling in endothelial progenitor cells. *FASEB J* 2005;**19**:974–976.
4. Hill JM, Zalos G, Halcox JP, Schenke WH, Waclawiw MA, Quyyumi AA *et al.* Circulating endothelial progenitor cells, vascular function, and cardiovascular risk. *N Engl J Med* 2003;**348**:593–600.
5. Moromizato Y, Stechschulte S, Miyamoto K, Murata T, Tsujikawa A, Joussen AM *et al.* CD18 and ICAM-1-dependent corneal neovascularization and inflammation after limbal injury. *Am J Pathol* 2000;**157**:1277–1281.
6. Sainz J, Sata M. CXCR4, a key modulator of vascular progenitor cells. *Arterioscler Thromb Vasc Biol* 2007;**27**:263–265.
7. Shiba Y, Takahashi M, Yoshioka T, Yajima N, Morimoto H, Izawa A *et al.* M-CSF accelerates neointimal formation in the early phase after vascular injury in mice: the critical role of the SDF-1-CXCR4 system. *Arterioscler Thromb Vasc Biol* 2007;**27**:283–289.
8. Satoh K, Kagaya Y, Nakano M, Ito Y, Ohta J, Tada H *et al.* Important role of endogenous erythropoietin system in recruitment of endothelial progenitor cells in hypoxia-induced pulmonary hypertension in mice. *Circulation* 2006;**113**:1442–1450.
9. Nagaya N, Kangawa K, Kanda M, Uematsu M, Horio T, Fukuyama N *et al.* Hybrid cell-gene therapy for pulmonary hypertension based on phagocytosing action of endothelial progenitor cells. *Circulation* 2003;**108**:889–895.
10. Zhao YD, Courtman DW, Deng Y, Kugathasan L, Zhang Q, Stewart DJ. Rescue of monocrotaline-induced pulmonary arterial hypertension using bone marrow-derived endothelial-like progenitor cells: efficacy of combined cell and eNOS gene therapy in established disease. *Circ Res* 2005;**96**:442–450.
11. Bull TM, Golpon H, Hebbel RP, Solovey A, Cool CD, Tuder RM *et al.* Circulating endothelial cells in pulmonary hypertension. *Thromb Haemost* 2003;**90**:698–703.
12. Nishimura T, Faul JL, Berry GJ, Vaszar LT, Qiu D, Pearl RG *et al.* Simvastatin attenuates smooth muscle neointimal proliferation and pulmonary hypertension in rats. *Am J Respir Crit Care Med* 2002;**166**:1403–1408.
13. Newman JH, Fanburg BL, Archer SL, Badesch DB, Barst RJ, Garcia JG *et al.* Pulmonary arterial hypertension: future directions: report of a

National Heart, Lung and Blood Institute/Office of Rare Diseases workshop. *Circulation* 2004;**109**:2947–2952.
14. Murata T, Kinoshita K, Hori M, Kuwahara M, Tsubone H, Karaki H *et al.* Statin protects endothelial nitric oxide synthase activity in hypoxia-induced pulmonary hypertension. *Arterioscler Thromb Vasc Biol* 2005;**25**:2335–2342.
15. Dimmeler S, Aicher A, Vasa M, Mildner-Rihm C, Adler K, Tiemann M *et al.* HMG-CoA reductase inhibitors (statins) increase endothelial progenitor cells via the PI 3-kinase/Akt pathway. *J Clin Invest* 2001;**108**:391–397.
16. Llevadot J, Murasawa S, Kureishi Y, Uchida S, Masuda H, Kawamoto A *et al.* HMG-CoA reductase inhibitor mobilizes bone marrow–derived endothelial progenitor cells. *J Clin Invest* 2001;**108**:399–405.
17. Hristov M, Fach C, Becker C, Heussen N, Liehn EA, Blindt R *et al.* Reduced numbers of circulating endothelial progenitor cells in patients with coronary artery disease associated with long-term statin treatment. *Atherosclerosis* 2007;**192**:413–420.
18. Urbich C, Dernbach E, Zeiher AM, Dimmeler S. Double-edged role of statins in angiogenesis signaling. *Circ Res* 2002;**90**:737–744.
19. Simper D, Stalboerger PG, Panetta CJ, Wang S, Caplice NM. Smooth muscle progenitor cells in human blood. *Circulation* 2002;**106**:1199–1204.
20. Sugiyama S, Kugiyama K, Nakamura S, Kataoka K, Aikawa M, Shimizu K *et al.* Characterization of smooth muscle-like cells in circulating human peripheral blood. *Atherosclerosis* 2006;**187**:351–362.
21. Sata M, Saiura A, Kunisato A, Tojo A, Okada S, Tokuhisa T *et al.* Hematopoietic stem cells differentiate into vascular cells that participate in the pathogenesis of atherosclerosis. *Nat Med* 2002;**8**:403–409.
22. Zhang LN, Wilson DW, da Cunha V, Sullivan ME, Vergona R, Rutledge JC *et al.* Endothelial NO synthase deficiency promotes smooth muscle progenitor cells in association with upregulation of stromal cell-derived factor-1alpha in a mouse model of carotid artery ligation. *Arterioscler Thromb Vasc Biol* 2006;**26**:765–772.
23. Caplice NM, Bunch TJ, Stalboerger PG, Wang S, Simper D, Miller DV *et al.* Smooth muscle cells in human coronary atherosclerosis can originate from cells administered at marrow transplantation. *Proc Natl Acad Sci USA* 2003;**100**:4754–4759.
24. Hashimoto N, Jin H, Liu T, Chensue SW, Phan SH. Bone marrow-derived progenitor cells in pulmonary fibrosis. *J Clin Invest* 2004;**113**:243–252.
25. Davie NJ, Crossno JT Jr, Frid MG, Hofmeister SE, Reeves JT, Hyde DM *et al.* Hypoxia-induced pulmonary artery adventitial remodeling and neovascularization: contribution of progenitor cells. *Am J Physiol Lung Cell Mol Physiol* 2004;**286**:L668–L678.
26. Stenmark KR, Davie NJ, Reeves JT, Frid MG. Hypoxia, leukocytes, and the pulmonary circulation. *J Appl Physiol* 2005;**98**:715–721.
27. Frid MG, Brunetti JA, Burke DL, Carpenter TC, Davie NJ, Reeves JT *et al.* Hypoxia-induced pulmonary vascular remodeling requires recruitment of circulating mesenchymal precursors of a monocyte/macrophage lineage. *Am J Pathol* 2006;**168**:659–669.
28. Hayashida K, Fujita J, Miyake Y, Kawada H, Ando K, Ogawa S *et al.* Bone marrow-derived cells contribute to pulmonary vascular remodeling in hypoxia-induced pulmonary hypertension. *Chest* 2005;**127**:1793–1798.
29. Zambrowicz BP, Imamoto A, Fiering S, Herzenberg LA, Kerr WG, Soriano P. Disruption of overlapping transcripts in the ROSA beta geo 26 gene trap strain leads to widespread expression of beta-galactosidase in mouse embryos and hematopoietic cells. *Proc Natl Acad Sci USA* 1997;**94**:3789–3794.
30. Assenmacher M, Manz R, Miltenyi S, Scheffold A, Radbruch A. Fluorescence-activated cytometry cell sorting based on immunological recognition. *Clin Biochem* 1995;**28**:39–40.
31. Jin DK, Shido K, Kopp HG, Petit I, Shmelkov SV, Young LM *et al.* Cytokine-mediated deployment of SDF-1 induces revascularization through recruitment of CXCR4+ hemangiocytes. *Nat Med* 2006;**12**:557–567.
32. Grunewald M, Avraham I, Dor Y, Bachar-Lustig E, Itin A, Jung S *et al.* VEGF-induced adult neovascularization: recruitment, retention, and role of accessory cells. *Cell* 2006;**124**:175–189.
33. Chavakis E, Aicher A, Heeschen C, Sasaki K, Kaiser R, El Makhfi N *et al.* Role of beta2-integrins for homing and neovascularization capacity of endothelial progenitor cells. *J Exp Med* 2005;**201**:63–72.
34. Yoder MC, Mead LE, Prater D, Krier TR, Mroueh KN, Li F *et al.* Redefining endothelial progenitor cells via clonal analysis and hematopoietic stem/progenitor cell principals. *Blood* 2007;**109**:1801–1809.
35. Sahara M, Sata M, Morita T, Nakamura K, Hirata Y, Nagai R. Diverse contribution of bone marrow-derived cells to vascular remodeling associated with pulmonary arterial hypertension and arterial neointimal formation. *Circulation* 2007;**115**:509–517.
36. Short M, Nemenoff RA, Zawada WM, Stenmark KR, Das M. Hypoxia induces differentiation of pulmonary artery adventitial fibroblasts into myofibroblasts. *Am J Physiol Cell Physiol* 2004;**286**:C416–C425.
37. Nishimura T, Vaszar LT, Faul JL, Zhao G, Berry GJ, Shi L *et al.* Simvastatin rescues rats from fatal pulmonary hypertension by inducing apoptosis of neointimal smooth muscle cells. *Circulation* 2003;**108**:1640–1655.
38. Girgis RE, Li D, Zhan X, Garcia JG, Tuder RM, Hassoun PM *et al.* Attenuation of chronic hypoxic pulmonary hypertension by simvastatin. *Am J Physiol Heart Circ Physiol* 2003;**285**:H938–H945.
39. Voelkel NF, Tuder RM. Hypoxia-induced pulmonary vascular remodeling: a model for what human disease? *J Clin Invest* 2000;**106**:733–738.
40. Ceradini DJ, Kulkarni AR, Callaghan MJ, Tepper OM, Bastidas N, Kleinman ME *et al.* Progenitor cell trafficking is regulated by hypoxic gradients through HIF-1 induction of SDF-1. *Nat Med* 2004;**10**:858–864.
41. Schober A, Knarren S, Lietz M, Lin EA, Weber C. Crucial role of stromal cell-derived factor-1alpha in neointima formation after vascular injury in apolipoprotein E-deficient mice. *Circulation* 2003;**108**:2491–2497.
42. Kusuyama T, Omura T, Nishiya D, Enomoto S, Matsumoto R, Murata T *et al.* The effects of HMG-CoA reductase inhibitor on vascular progenitor cells. *J Pharmacol Sci* 2006;**101**:344–349.
43. Fukumoto Y, Libby P, Rabkin E, Hill CC, Enomoto M, Hirouchi Y *et al.* Statins alter smooth muscle cell accumulation and collagen content in established atheroma of watanabe heritable hyperlipidemic rabbits. *Circulation* 2001;**103**:993–999.
44. Foody JM, Shah R, Galusha D, Masoudi FA, Havranek EP, Krumholz HM. Statins and mortality among elderly patients hospitalized with heart failure. *Circulation* 2006;**113**:1086–1092.
45. Pasceri V, Patti G, Nusca A, Pristipino C, Richichi G, Di Sciascio G. Randomized trial of atorvastatin for reduction of myocardial damage during coronary intervention: results from the ARMYDA (Atorvastatin for Reduction of MYocardial Damage during Angioplasty) study. *Circulation* 2004;**110**:674–678.
46. Kao PN. Simvastatin treatment of pulmonary hypertension: an observational case series. *Chest* 2005;**127**:1446–1452.